FINITE GEOMETRIES: OTHER NOTABLE EXAMPLES

Metod Saniga

Astronomical Institute
Slovak Academy of Sciences
SK-05960 Tatranská Lomnica
Slovak Republic

(msaniga@astro.sk)

Department of Algebra, Geometry and Math Education, FMPI,
Comenius University, Bratislava

February 23, 2018

Overview

- Non-unimodular points
- Veldkamp spaces and...
- ...binary Segre varieties
- ...Cayley-Dickson algebras
- ...Dynkin diagrams
- Pseudo-Veldkamp spaces

Non-unimodular points

Projective ring line: admissible pair

Consider a(n associative) ring with unity, R, and $GL(2, R)$, the general linear group of invertible two-by-two matrices with entries in R.

A pair $(a, b) \in R^2$ is called *admissible* over R if there exist $c, d \in R$ such that

$$\begin{pmatrix} a & b \\ c & d \end{pmatrix} \in GL(2, R), \tag{1}$$

which for commutative R reads

$$\det \begin{pmatrix} a & b \\ c & d \end{pmatrix} \in R^*. \tag{2}$$

A pair $(a, b) \in R^2$ is called *unimodular* over R if there exist $c, d \in R$ such that $ac + bd = 1$.

For finite rings: admissible $\Leftrightarrow$ unimodular.

Projective ring line: free cyclic submodules

$R(a,b)$, a (left) *cyclic submodule* of R^2:
$R(a,b) = \{(\alpha a, \alpha b) | (a,b) \in R^2, \alpha \in R\}$.

A cyclic submodule $R(a,b)$ is called *free* if the mapping $\alpha \mapsto (\alpha a, \alpha b)$ is injective, i. e., if all $(\alpha a, \alpha b)$ are distinct.

Crucial property: if (a,b) is admissible, then $R(a,b)$ is free.

However, there also exist rings yielding free cyclic submodules (FCSs) containing *no* admissible pairs!

Generalizing the definition of $P(R)$, the *projective line over* R:
$P(R) = \{R(a,b) \subset R^2 | R(a,b) \ \ \textit{free}\}$.

Non-unimodular FCS's – ternions

The smallest order when they appear is the *smallest ring of ternions* $R_\diamondsuit$, i. e. the ring isomorphic to the one of upper triangular two-by-two matrices over the Galois field of two elements:

$$R_\diamondsuit \equiv \left\{ \begin{pmatrix} a & b \\ 0 & c \end{pmatrix} \mid \; a, b, c \in GF(2) \right\}. \tag{3}$$

Explicitly:

$$0 \equiv \begin{pmatrix} 0 & 0 \\ 0 & 0 \end{pmatrix}, \quad 1 \equiv \begin{pmatrix} 1 & 0 \\ 0 & 1 \end{pmatrix}, \quad 2 \equiv \begin{pmatrix} 1 & 1 \\ 0 & 1 \end{pmatrix}, \quad 3 \equiv \begin{pmatrix} 1 & 1 \\ 0 & 0 \end{pmatrix},$$

$$4 \equiv \begin{pmatrix} 0 & 0 \\ 0 & 1 \end{pmatrix}, \quad 5 \equiv \begin{pmatrix} 1 & 0 \\ 0 & 0 \end{pmatrix}, \quad 6 \equiv \begin{pmatrix} 0 & 1 \\ 0 & 0 \end{pmatrix}, \quad 7 \equiv \begin{pmatrix} 0 & 1 \\ 0 & 1 \end{pmatrix}.$$

Non-unimodular FCS's – ternions

Table: Addition (*left*) and multiplication (*right*) in $R_{\diamondsuit}$.

$+$	0	1	2	3	4	5	6	7
0	0	1	2	3	4	5	6	7
1	1	0	6	7	5	4	2	3
2	2	6	0	4	3	7	1	5
3	3	7	4	0	2	6	5	1
4	4	5	3	2	0	1	7	6
5	5	4	7	6	1	0	3	2
6	6	2	1	5	7	3	0	4
7	7	3	5	1	6	2	4	0

$\times$	0	1	2	3	4	5	6	7
0	0	0	0	0	0	0	0	0
1	0	1	2	3	4	5	6	7
2	0	2	1	3	7	5	6	4
3	0	3	5	3	6	5	6	0
4	0	4	4	0	4	0	0	4
5	0	5	3	3	0	5	6	6
6	0	6	6	0	6	0	0	6
7	0	7	7	0	7	0	0	7

Non-unimodular FCS's – ternions

36 *uni*modular vectors which generate 18 different FCS's:

$$
\begin{aligned}
R_\diamondsuit(1,0) = R_\diamondsuit(2,0) &= \{(0,0),(6,0),(4,0),(7,0),(5,0),(3,0),(2,0),(1,0)\},\\
R_\diamondsuit(1,6) = R_\diamondsuit(2,6) &= \{(0,0),(6,0),(4,0),(7,0),(5,6),(3,6),(2,6),(1,6)\},\\
R_\diamondsuit(1,3) = R_\diamondsuit(2,3) &= \{(0,0),(6,0),(4,0),(7,0),(5,3),(3,3),(2,3),(1,3)\},\\
R_\diamondsuit(1,5) = R_\diamondsuit(2,5) &= \{(0,0),(6,0),(4,0),(7,0),(5,5),(3,5),(2,5),(1,5)\},\\
R_\diamondsuit(7,3) = R_\diamondsuit(4,3) &= \{(0,0),(6,0),(4,0),(7,0),(0,3),(6,3),(4,3),(7,3)\},\\
R_\diamondsuit(7,5) = R_\diamondsuit(4,5) &= \{(0,0),(6,0),(4,0),(7,0),(0,5),(6,5),(4,5),(7,5)\},\\
R_\diamondsuit(1,7) = R_\diamondsuit(2,4) &= \{(0,0),(6,6),(4,4),(7,7),(5,6),(3,0),(2,4),(1,7)\},\\
R_\diamondsuit(1,4) = R_\diamondsuit(2,7) &= \{(0,0),(6,6),(4,4),(7,7),(5,0),(3,6),(2,7),(1,4)\},\\
R_\diamondsuit(1,1) = R_\diamondsuit(2,2) &= \{(0,0),(6,6),(4,4),(7,7),(5,5),(3,3),(2,2),(1,1)\},\\
R_\diamondsuit(1,2) = R_\diamondsuit(2,1) &= \{(0,0),(6,6),(4,4),(7,7),(5,3),(3,5),(2,1),(1,2)\},\\
R_\diamondsuit(4,1) = R_\diamondsuit(7,2) &= \{(0,0),(6,6),(4,4),(7,7),(0,5),(6,3),(7,2),(4,1)\},\\
R_\diamondsuit(7,1) = R_\diamondsuit(4,2) &= \{(0,0),(6,6),(4,4),(7,7),(0,3),(6,5),(4,2),(7,1)\},\\
R_\diamondsuit(3,7) = R_\diamondsuit(3,4) &= \{(0,0),(0,6),(0,4),(0,7),(3,0),(3,6),(3,4),(3,7)\},\\
R_\diamondsuit(5,7) = R_\diamondsuit(5,4) &= \{(0,0),(0,6),(0,4),(0,7),(5,0),(5,6),(5,4),(5,7)\},\\
R_\diamondsuit(5,1) = R_\diamondsuit(5,2) &= \{(0,0),(0,6),(0,4),(0,7),(5,5),(5,3),(5,2),(5,1)\},\\
R_\diamondsuit(3,1) = R_\diamondsuit(3,2) &= \{(0,0),(0,6),(0,4),(0,7),(3,5),(3,3),(3,2),(3,1)\},\\
R_\diamondsuit(6,1) = R_\diamondsuit(6,2) &= \{(0,0),(0,6),(0,4),(0,7),(6,5),(6,3),(6,2),(6,1)\},\\
R_\diamondsuit(0,1) = R_\diamondsuit(0,2) &= \{(0,0),(0,6),(0,4),(0,7),(0,5),(0,3),(0,2),(0,1)\},
\end{aligned}
$$

and

Non-unimodular FCS's – ternions

6 *non*-unimodular vectors giving rise to 3 distinct FCS's:

$$R_\diamond(4,6) = R_\diamond(7,6) = \{(0,0),(6,0),(0,6),(6,6),(4,0),(7,0),(7,6),(4,6)\},$$
$$R_\diamond(4,7) = R_\diamond(7,4) = \{(0,0),(6,0),(0,6),(6,6),(4,4),(7,7),(7,4),(4,7)\},$$
$$R_\diamond(6,4) = R_\diamond(6,7) = \{(0,0),(6,0),(0,6),(6,6),(0,4),(0,7),(6,7),(6,4)\}.$$

Non-unimodular FCS's – ternions

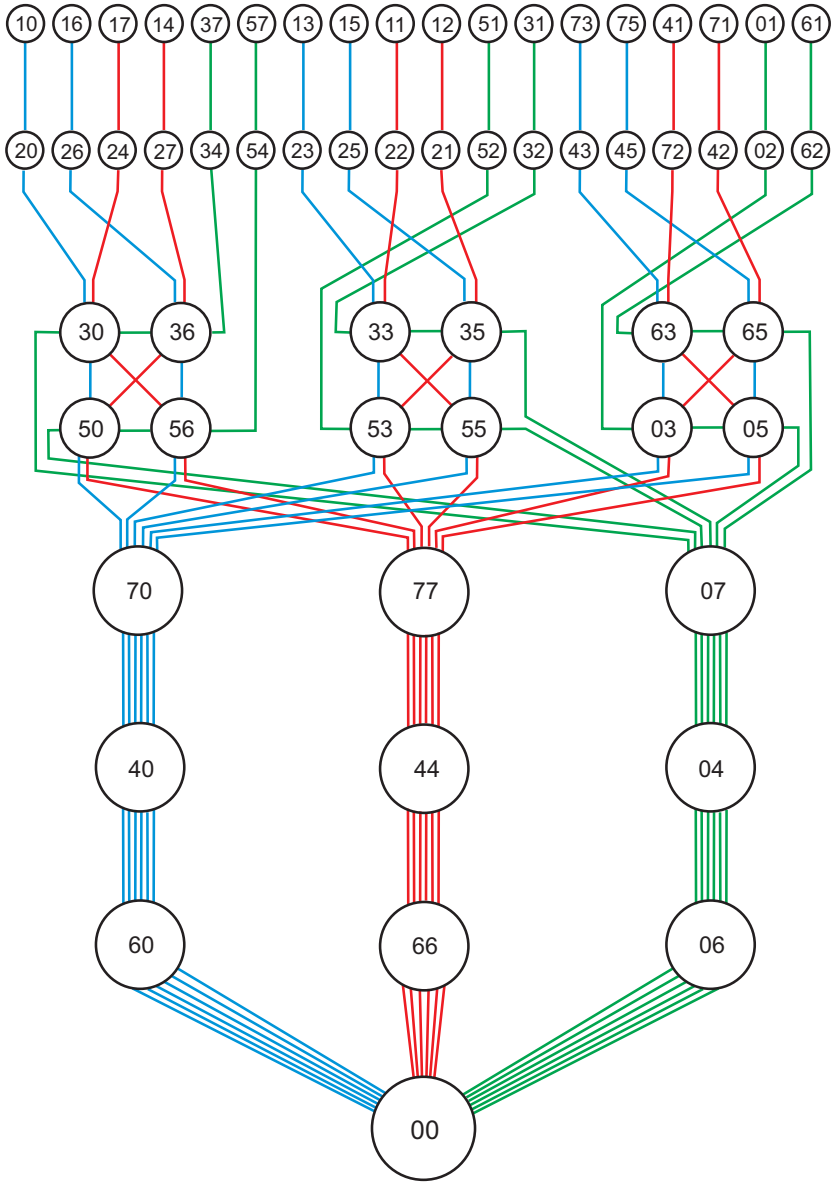

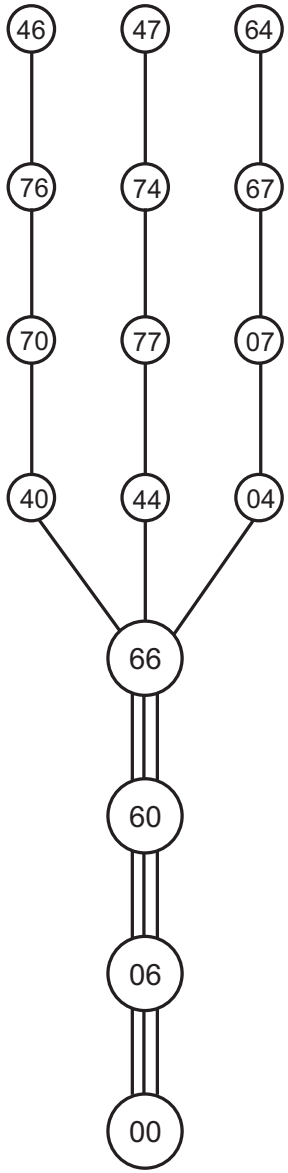

Non-unimodular FCS's – ternions

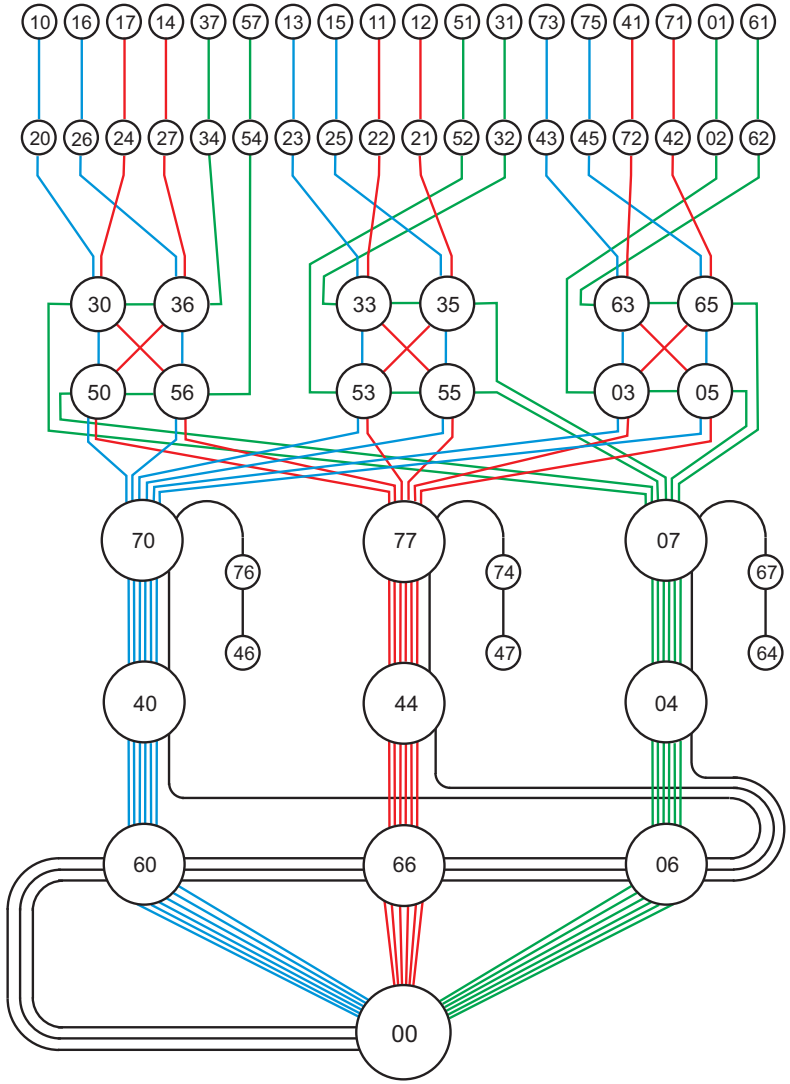

Non-unimodular FCS's – other rings

Our preliminary analysis of a few small cases indicates that this non-unimodular part has in some cases the structure that it homomorphic to a "standard" line. Let us introduce a couple of examples.

The first one is the line defined over a non-commutative ring of order 16 having 12 zero-divisors (a 16/12 ring), whose non-unimodular part is homomorphic to the line defined over $\mathcal{Z}_4$ or $\mathcal{Z}_2[x]/\langle x^2 \rangle$.

The other example is furnished by the line defined over a non-commutative ring of the 16/14 type, whose non-unimodular part is homomorphic to the line defined over $\mathcal{Z}_2 \times \mathcal{Z}_2$.

Both the cases are illustrated on the next figure; here, all crossed circles represent vectors that do not lie on any FCS generated by unimodular pairs ("outliers"), with those of them that are half-filled not generating FCSs.

Non-unimodular FCS's – other rings

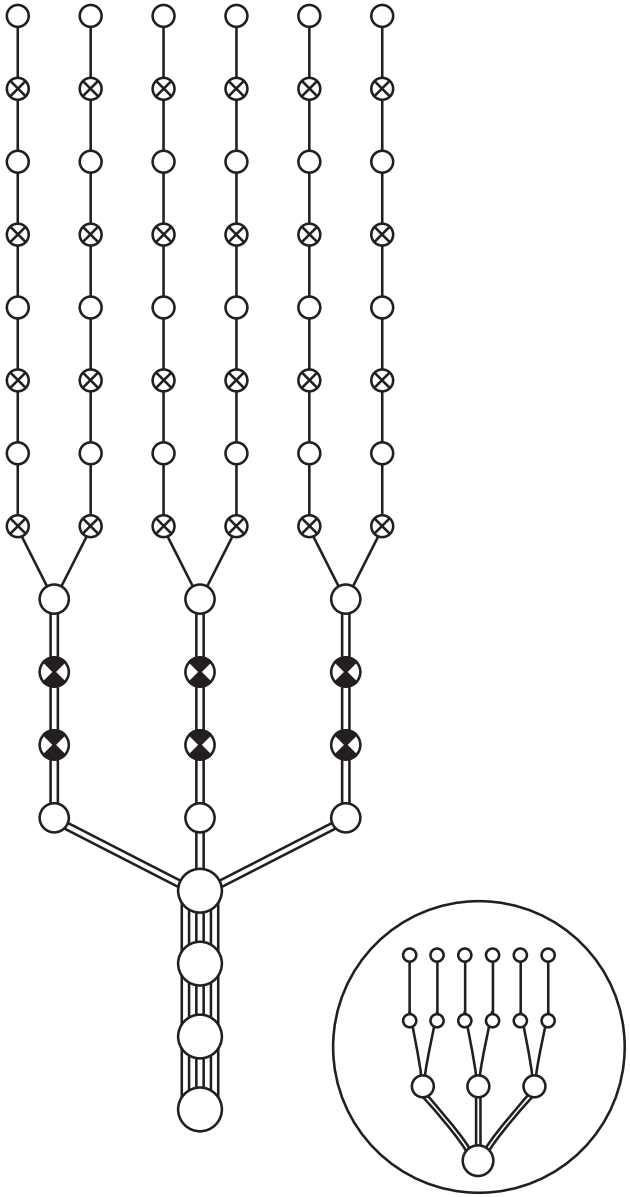

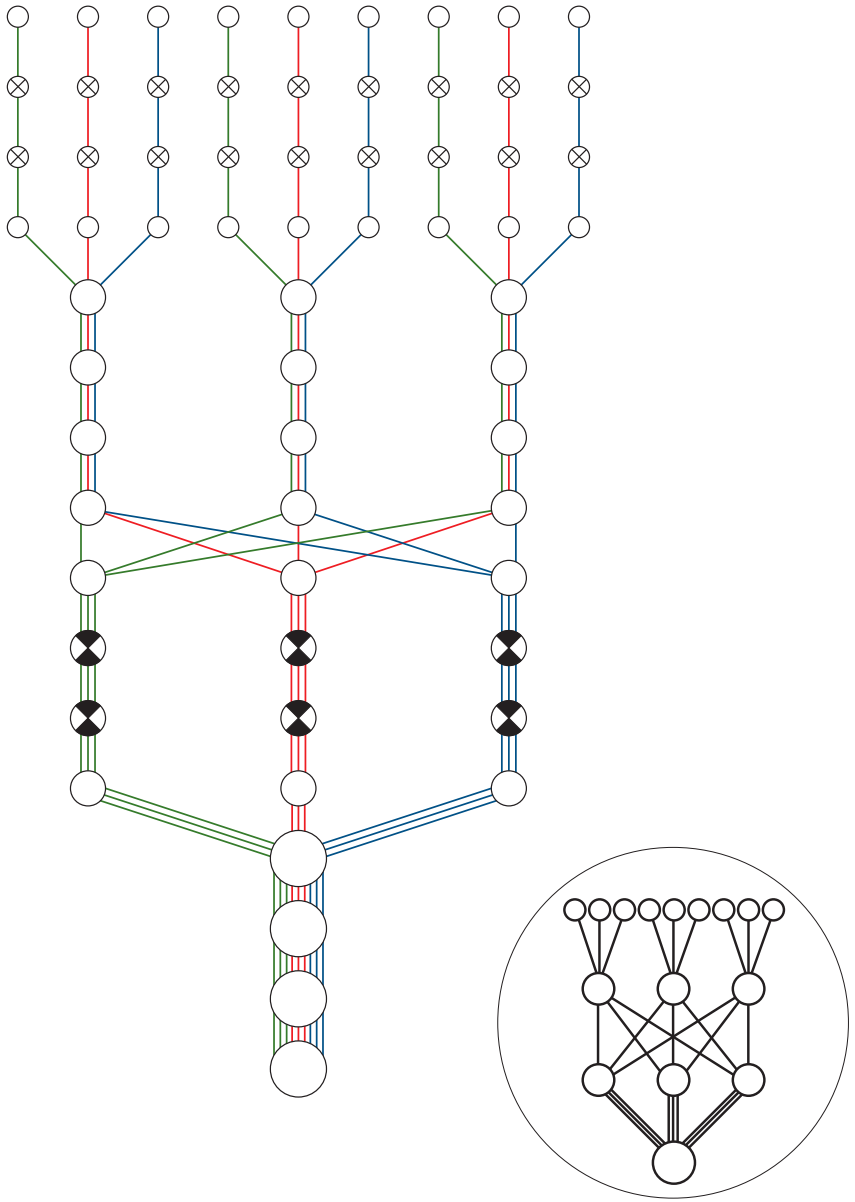

Non-unimodular FCS's – other rings

The following table shows that up to order 27 there exists only one line whose non-unimodular part is *not* homorphic to a ring line; here the first column gives the ring type, the second column features the number of outliers (total vs generating FCSs) and the last column lists the type of homomorphic image of the non-unimodular part.

8/6	6/6	$P(\mathcal{Z}_2)$
16/12a	30/24	$P(\mathcal{Z}_4)$ or $P(\mathcal{Z}_2[x]/\langle x^2\rangle)$
16/12b	42/36	not a ring line
16/14	24/18	$P(\mathcal{Z}_2 \times \mathcal{Z}_2)$
24/20	54/48	$P(\mathcal{Z}_6) \simeq P(\mathcal{Z}_2 \times \mathcal{Z}_3)$
27/15	48/48	$P(\mathcal{Z}_3)$

Non-unimodular FCS's – some more physics?

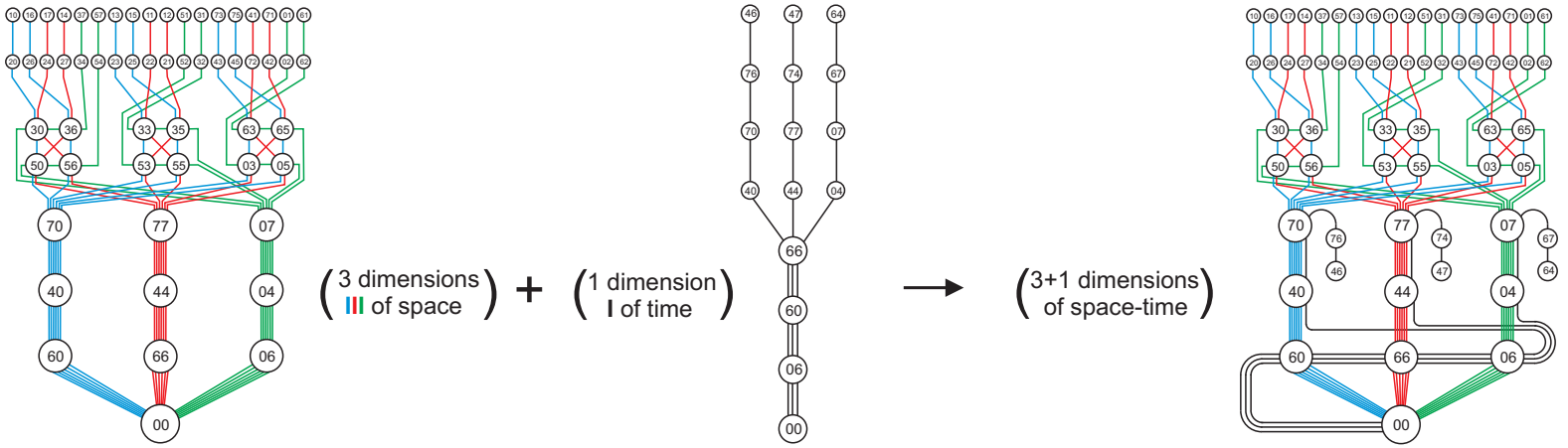

Couldn't, then, our universe simply be a projective ring line of a huge, yet still finite order (structured as shown in the table below), unjustly neglected and inadequately hidden under a variety of disguises like a pseudo-Riemannian manifold, a world of strings and branes, etc.?

Space-time	Projective Ring Line of a Very Large Order
Space	Set of Unimodular Points
Time	Set of Non-Unimodular Points
3D of Space	Three Unique Maximum Sets of Mutually Neighbour Unimodulars
1D of Time	Non-Unimodulars Form One Maximum Set of Mutually Neighbours
Arrow of Time	Condensation Phenomenon

'Fano-snowflake'

Let's now have a look at

- *free* left cyclic submodules generated by
- *non*-unimodular *triples* of elements from $R_{\diamondsuit}$.

We find altogether

- 42 *non*-unimodular triples of elements generating
- 21 distinct free left cyclic submodules:

'Fano-snowflake'

$$R_\diamond(4,6,7) = \{(0,0,0),(4,6,7),(7,6,4),(6,6,0),(4,0,4),(0,6,6),(6,0,6),(7,0,7)\},$$
$$R_\diamond(4,7,6) = \{(0,0,0),(4,7,6),(7,4,6),(6,0,6),(4,4,0),(0,6,6),(6,6,0),(7,7,0)\},$$
$$R_\diamond(6,4,7) = \{(0,0,0),(6,4,7),(6,7,4),(6,6,0),(0,4,4),(6,0,6),(0,6,6),(0,7,7)\},$$
$$R_\diamond(4,4,7) = \{(0,0,0),(4,4,7),(7,7,4),(6,6,0),(4,4,4),(0,0,6),(6,6,6),(7,7,7)\},$$
$$R_\diamond(4,7,4) = \{(0,0,0),(4,7,4),(7,4,7),(6,0,6),(4,4,4),(0,6,0),(6,6,6),(7,7,7)\},$$
$$R_\diamond(7,4,4) = \{(0,0,0),(7,4,4),(4,7,7),(0,6,6),(4,4,4),(6,0,0),(6,6,6),(7,7,7)\},$$
$$R_\diamond(4,4,6) = \{(0,0,0),(4,4,6),(7,7,6),(6,6,6),(4,4,0),(0,0,6),(6,6,0),(7,7,0)\},$$
$$R_\diamond(4,6,4) = \{(0,0,0),(4,6,4),(7,6,7),(6,6,6),(4,0,4),(0,6,0),(6,0,6),(7,0,7)\},$$
$$R_\diamond(6,4,4) = \{(0,0,0),(6,4,4),(6,7,7),(6,6,6),(0,4,4),(6,0,0),(0,6,6),(0,7,7)\},$$
$$R_\diamond(6,6,7) = \{(0,0,0),(6,6,7),(6,6,4),(6,6,0),(0,0,4),(6,6,6),(0,0,6),(0,0,7)\},$$
$$R_\diamond(6,7,6) = \{(0,0,0),(6,7,6),(6,4,6),(6,0,6),(0,4,0),(6,6,6),(0,6,0),(0,7,0)\},$$
$$R_\diamond(7,6,6) = \{(0,0,0),(7,6,6),(4,6,6),(0,6,6),(4,0,0),(6,6,6),(6,0,0),(7,0,0)\},$$
$$R_\diamond(0,6,7) = \{(0,0,0),(0,6,7),(0,6,4),(0,6,0),(0,0,4),(0,6,6),(0,0,6),(0,0,7)\},$$
$$R_\diamond(0,7,6) = \{(0,0,0),(0,7,6),(0,4,6),(0,0,6),(0,4,0),(0,6,6),(0,6,0),(0,7,0)\},$$
$$R_\diamond(0,4,7) = \{(0,0,0),(0,4,7),(0,7,4),(0,6,0),(0,4,4),(0,0,6),(0,6,6),(0,7,7)\},$$
$$R_\diamond(6,0,7) = \{(0,0,0),(6,0,7),(6,0,4),(6,0,0),(0,0,4),(6,0,6),(0,0,6),(0,0,7)\},$$
$$R_\diamond(7,0,6) = \{(0,0,0),(7,0,6),(4,0,6),(0,0,6),(4,0,0),(6,0,6),(6,0,0),(7,0,0)\},$$
$$R_\diamond(4,0,7) = \{(0,0,0),(4,0,7),(7,0,4),(6,0,0),(4,0,4),(0,0,6),(6,0,6),(7,0,7)\},$$
$$R_\diamond(6,7,0) = \{(0,0,0),(6,7,0),(6,4,0),(6,0,0),(0,4,0),(6,6,0),(0,6,0),(0,7,0)\},$$
$$R_\diamond(7,6,0) = \{(0,0,0),(7,6,0),(4,6,0),(0,6,0),(4,0,0),(6,6,0),(6,0,0),(7,0,0)\},$$
$$R_\diamond(4,7,0) = \{(0,0,0),(4,7,0),(7,4,0),(6,0,0),(4,4,0),(0,6,0),(6,6,0),(7,7,0)\}.$$

‘Fano-snowflake’

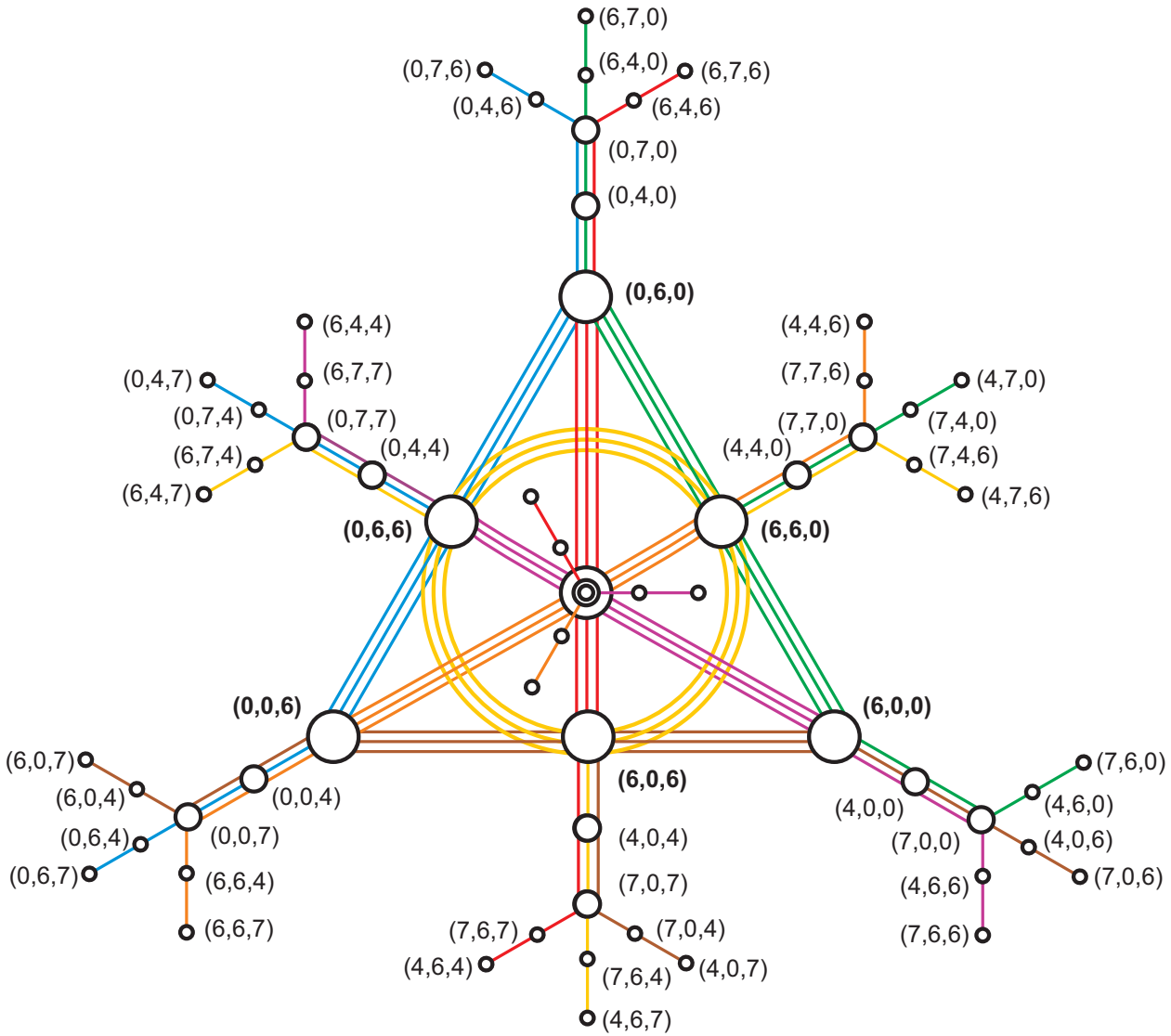

‘Fano-snowflake’

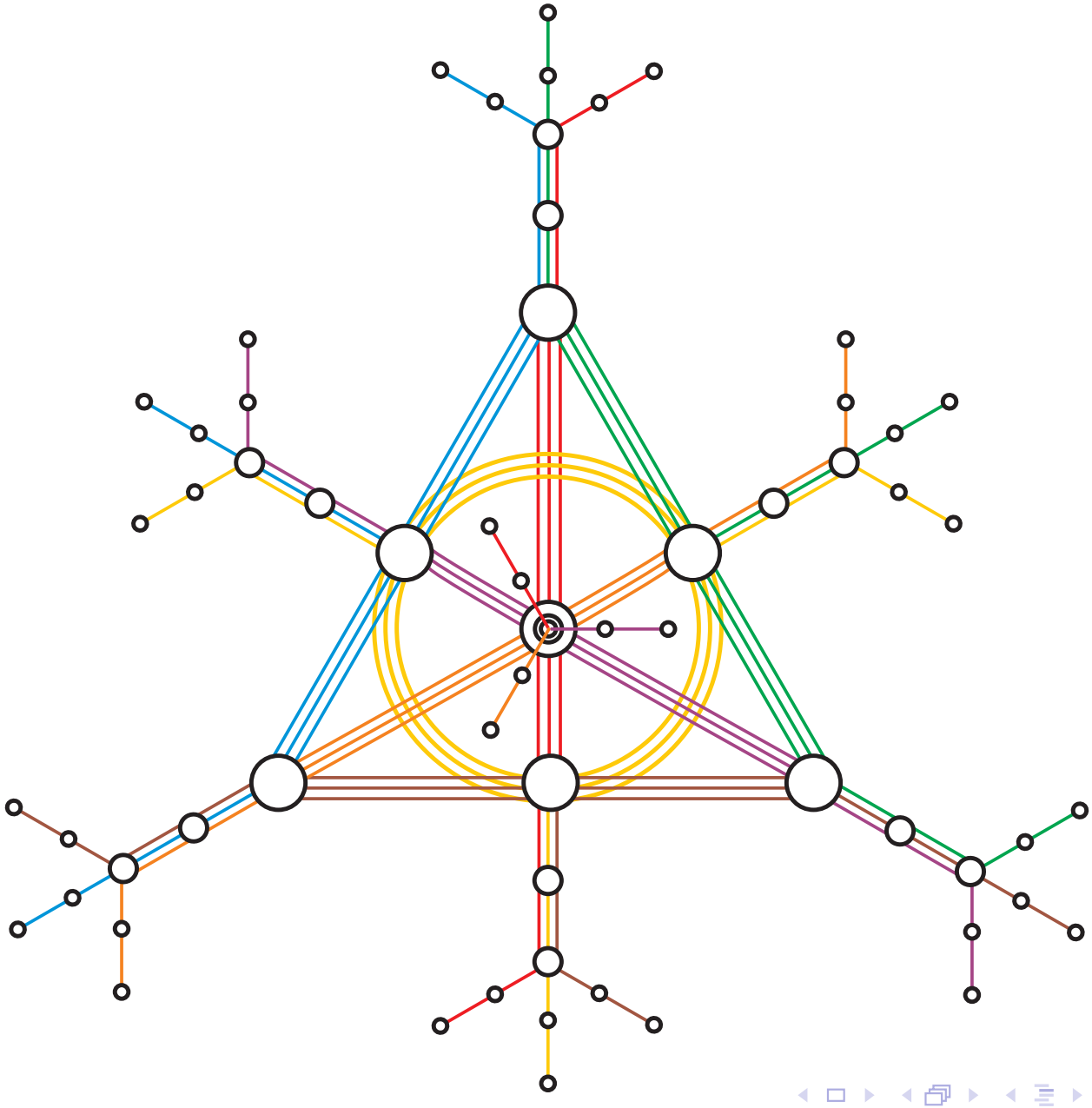

Generalization of 'Fano-snowflake'

For a general ring of ternions, i. e. a ring of upper triangular two-by-two matrices over

- GF(q),

and non-unimodular

- $(n+1)$-tuples

of elements, the corresponding geometry features

- PG(n, q)

in the middle of the 'snow-flake.'

Veldkamp spaces and...

Veldkamp space – definition

Given a point-line incidence geometry $\Gamma(P, L)$, a *geometric hyperplane* of $\Gamma(P, L)$ is a subset of its point set such that a line of the geometry is

- either *fully* contained in the subset
- or has with it just a *single* point in common.

The *Veldkamp* space of $\Gamma(P, L)$, $\mathcal{V}(\Gamma)$, is the space in which

- a point is a geometric hyperplane of Γ and
- a line is the collection $H'H''$ of all geometric hyperplanes H of Γ such that $H' \cap H'' = H' \cap H = H'' \cap H$ or $H = H', H''$, where H' and H'' are distinct points of $\mathcal{V}(\Gamma)$.

For a $\Gamma(P, L)$ with *three* points on a line, all Veldkamp lines are of the form $\{H', H'', \overline{H' \Delta H''}\}$ where $\overline{H' \Delta H''}$ is the complement of symmetric difference of H' and H'', i. e. they form a vector space over GF(2).

$\mathcal{V}(\mathrm{GQ}(2,2)) \simeq \mathrm{PG}(4,2)$

Its 31 points

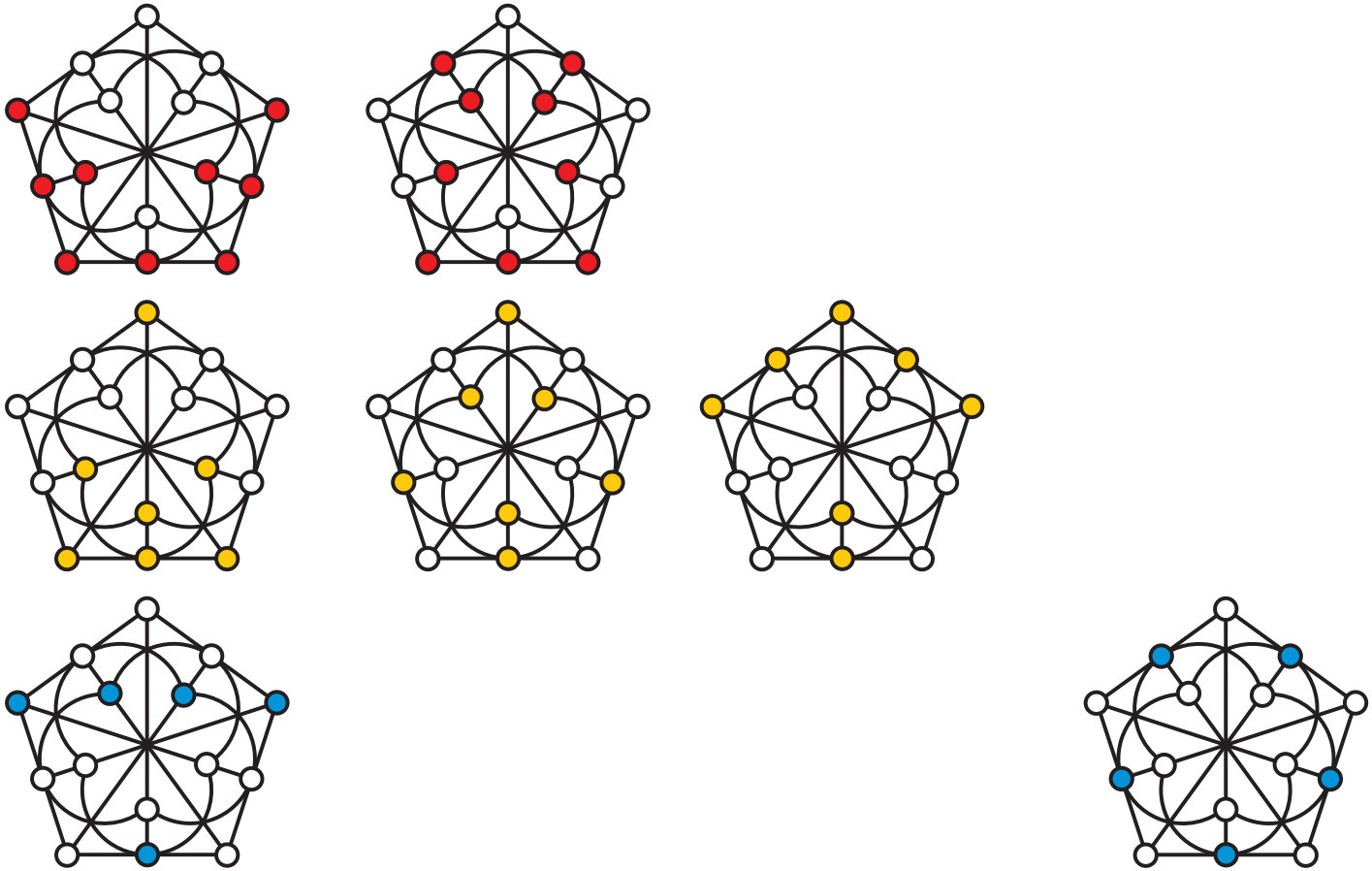

$\mathcal{V}(GQ(2,2)) \simeq PG(4,2)$

And its 155 lines

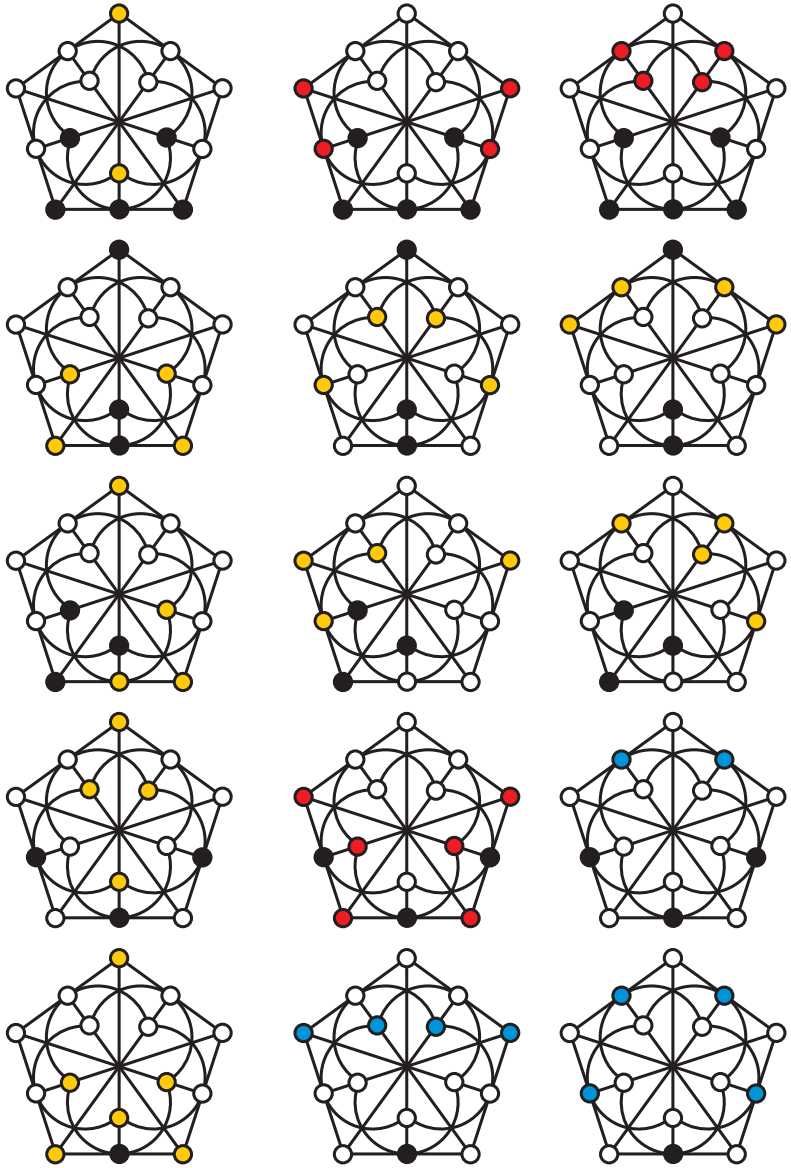

$\mathcal{V}(\mathrm{GQ}(2,2)) \simeq \mathrm{PG}(4,2)$

Table: A succinct summary of the properties of the five different types of the lines of $\mathcal{V}(\mathrm{GQ}(2,2))$ in terms of the core (i. e., the set of points common to all the three hyperplanes forming a line) and the types of geometric hyperplanes featured by a generic line of a given type. The last column gives the total number of lines per each type.

Type	Core	Perps	Ovoids	Grids	#
I	Pentad	1	0	2	45
II	Collinear Triple	3	0	0	15
III	Tricentric Triad	3	0	0	20
IV	Unicentric Triad	1	1	1	60
V	Single Point	1	2	0	15

$\mathcal{V}(\mathrm{GQ}(2,4)) \simeq \mathrm{PG}(5,2)$

Its 63 points comprise 27 perps and 36 doilies.

Its 651 lines are of four distinct types:

Table: The properties of the four different types of the lines of $\mathcal{V}(\mathrm{GQ}(2,4))$ in terms of the common intersection and the types of geometric hyperplanes featured by a generic line of a given type. The last column gives the total number of lines per the corresponding type.

Type	Intersection	Perps	Doilies	(Ovoids)	Total
I	Line	3	0	(–)	45
II	Ovoid	2	1	(–)	216
III	Perp-set	1	2	(–)	270
IV	Grid	0	3	(–)	120

$\mathcal{V}(\mathrm{GQ}(2,4)) \simeq \mathrm{PG}(5,2)$

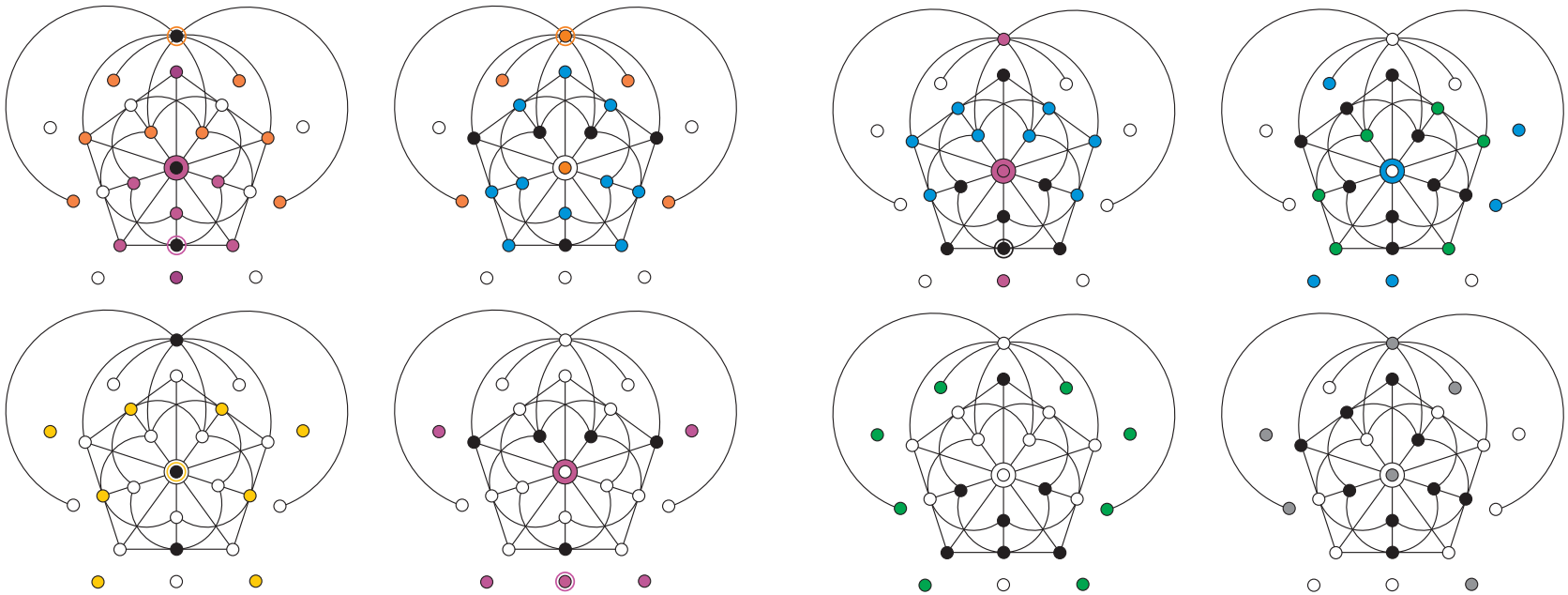

$\mathcal{V}(\mathrm{GQ}(4,2)) \simeq ???$

$\mathrm{GQ}(4,2)$,
associated with the classical group $\mathrm{PGU}_4(2)$,
can be represented by 45 points and 27 lines of
a non-degenerate *Hermitian* surface $H(3,4)$ in $\mathrm{PG}(3,4)$.

Its geometric hyperplanes are 45 perps of points and 200 ovoids.

As no $\mathrm{PG}(d,q)$ has $200 + 45 = 245$ points, $\mathcal{V}(\mathrm{GQ}(4,2))$ *can't* be isomorphic to any projective space!

$\mathcal{V}(\mathrm{GQ}(4,2))$

- is not even a partial linear space, although, remarkably,
- it contains a subspace isomorphic to $\mathrm{PG}(3,4)$.

No Veldkamp space

Do they also exist point-line incidence structures having

- no Veldkamp space?

Yes, they do.

One of the smallest non-trivial examples is

- the Moebius-Kantor 8_3-configuration.

...Segre varieties

Segre varieties: definition

Let $S_{(N)} \equiv PG(1,2) \times PG(1,2) \times \cdots \times PG(1,2)$ be a Segre variety that is N-fold direct product of projective lines of size three.

It is straightforward to see that the properties of

- Veldkamp *points* of $S_{(N)}$

are fully encoded in the properties of

- Veldkamp *lines* of $S_{(N-1)}$.

To this end, we shall use a slightly *generalized* notion of the Veldkamp space of Γ, $\mathcal{V}(\Gamma)$, which also includes Γ as the *extraordinary* geometric hyperplane and which features extraordinary Veldkamp lines, the latter being of type $\{H, H, \Gamma\}$.

- ord-$\mathcal{V}(S_{(N)}) \cong PG(2^N - 1, 2)$

Segre varieties: geometric hyperplanes of $S_{(2)}$

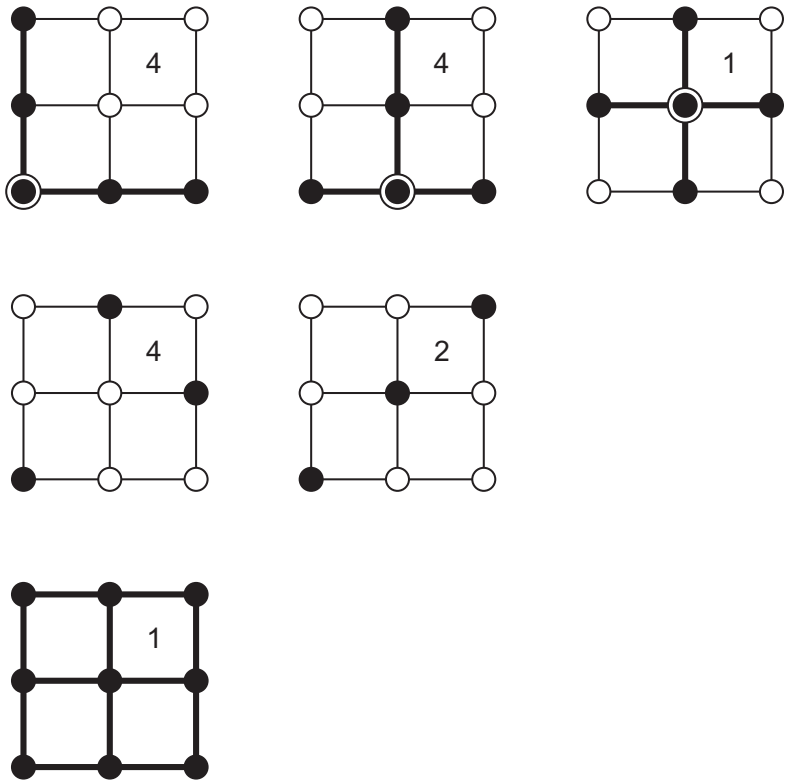

A diagrammatic representation of the types of geometric hyperplanes of $S_{(2)}$. The number attached to a subfigure indicates how many distinct copies of a given hyperplane one gets by rotating the subfigure around its center. The top row illustrates all 9 copies of type one hyperplane (a perp), the middle row all 6 copies of type two hyperplane (an ovoid) and, for the sake of completeness, the bottom row shows the extraordinary hyperplane. The encircled bullets in the top row denote deep points.)

Segre varieties: from $S_{(1)}$ to $S_{(2)}$

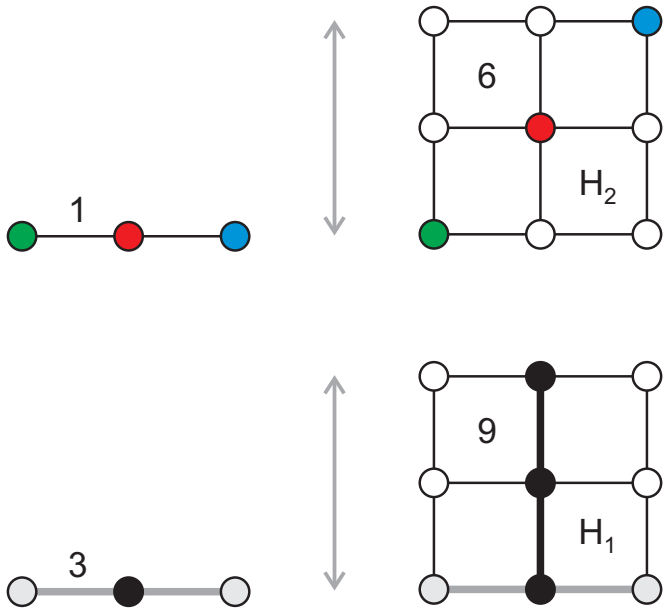

An illustration of the fact that the two types of geometric hyperplanes of $S_{(2)}$ (*right*) can be regarded as blow-ups of the Veldkamp lines of $S_{(1)}$ (*left*), or, *vice versa*, that a projection of a type two (*top right*) or type one (*bottom right*) hyperplane of $S_{(2)}$ onto a line of $S_{(2)}$ can be viewed, respectively, as the ordinary (*top left*) or an extraordinary (*bottom left*) Veldkamp line of $S_{(1)}$.

Segre varieties: geometric hyperplanes of $S_{(3)}$

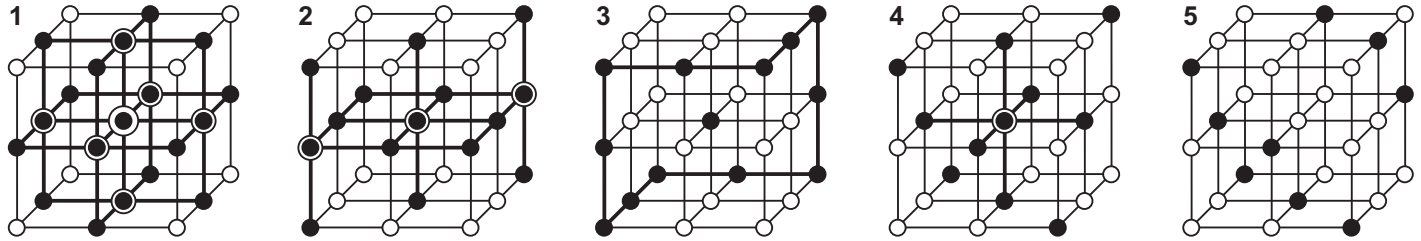

Tp	Ps	Ls	Points of Order				$S_{(2)}$'s of Type			VL	Crd	BS	W
			0	1	2	3	D	H_1	H_2				
1	19	15	0	0	12	7	3	6	0	I	27	2	1
2	15	9	0	6	6	3	1	6	2	II, 1	54	3	2
3	13	6	1	6	6	0	0	6	3	2	108	4	2
4	11	3	4	6	0	1	0	3	6	3	54	5	3
5	9	0	9	0	0	0	0	0	9	4	12	6	3

Regarding hyperplanes as points of the $PG(7,2)$ ($\cong$ ord-$\mathcal{V}(S_{(3)})$), it can be demonstrated that those points that correspond to hyperplanes of type one, two and four, and whose number totals to 135, all lie on a certain $\mathcal{Q}_0^+(7,2) \subset PG(7,2)$; note that these are exactly the three types whose members feature points of maximum order.
It is also worth mentioning here that these three hyperplane types in their totality correspond to the image, furnished by the Lagrangian Grassmannian of $LG(3,6)$ type, of the set of 135 maximal subspaces of $\mathcal{W}(5,2)$.

Segre varieties: from $S_{(2)}$ to $S_{(3)}$ – ordinary

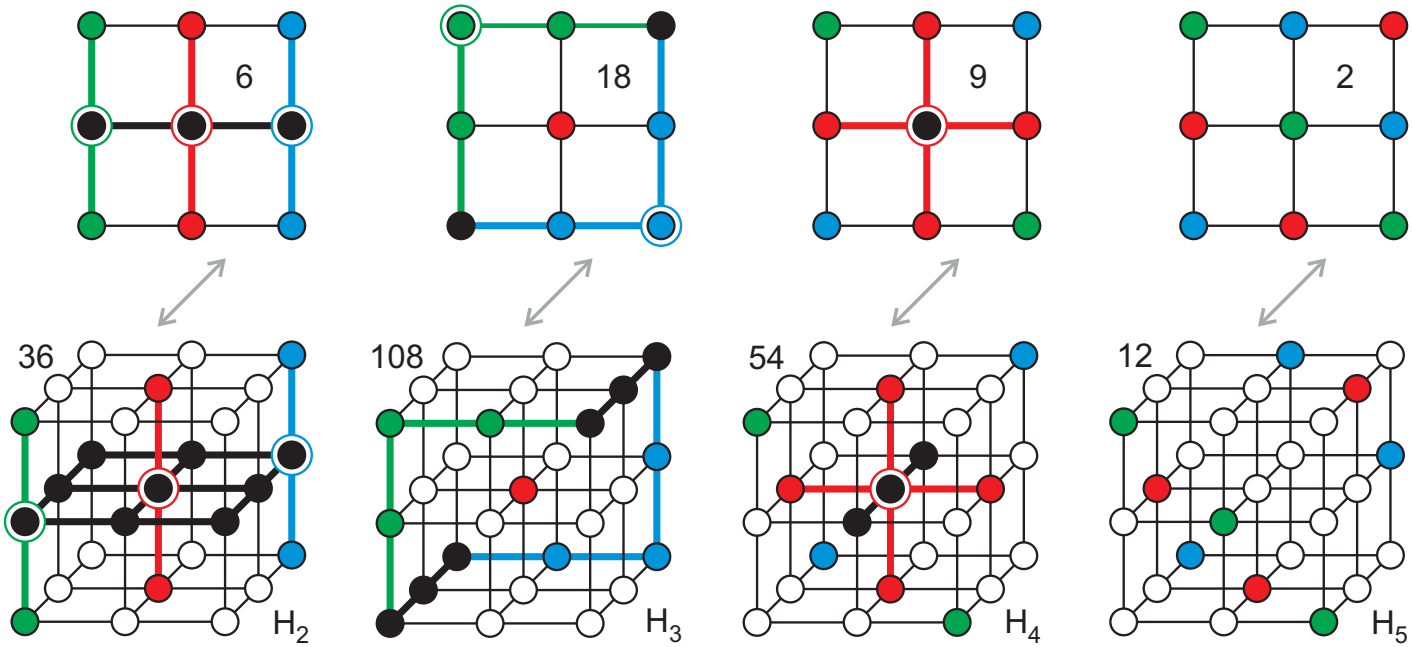

Top: – A descriptive illustration of the structure of the four distinct types (1 to 4, left to right) of ordinary Veldkamp lines of $S_{(2)}$; the three geometric hyperplanes comprising a Veldkamp line are distinguished by different colors, with the points and lines shared by all of them being colored black.
Bottom: – The four distinct types of geometric hyperplanes of $S_{(3)}$, as well as the number of copies per each type, we get by blowing-up Veldkamp lines of $S_{(2)}$ of the type shown above the particular subfigure.

Segre varieties: from $S_{(2)}$ to $S_{(3)}$ - extraordinary

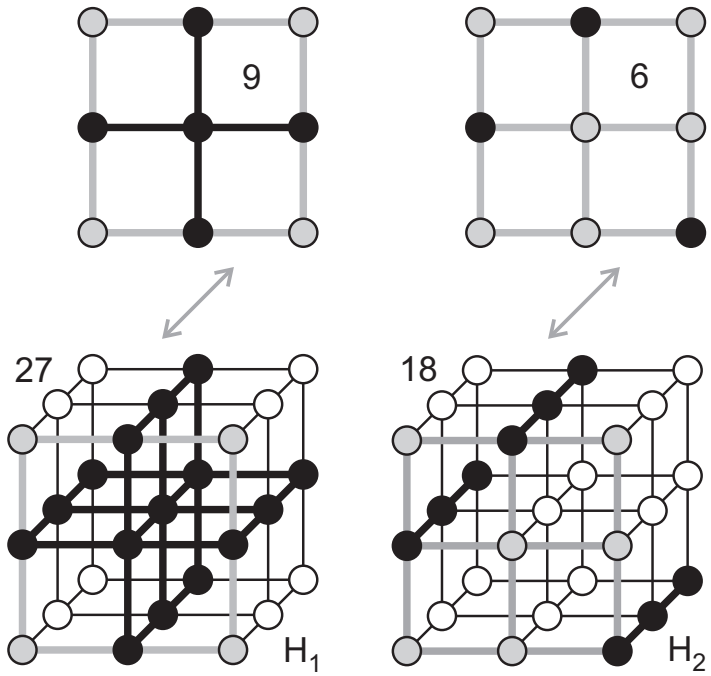

The same as in the previous figure, but for extraordinary Veldkamp lines of $S_{(2)}$ (*top*) and their $S_{(3)}$ blown-up cousins (*bottom*).

Segre varieties: (ordinary) Veldkamp lines of $S_{(3)}$)

Tp	Core		Composition					Crd
	Ps	Ls	H_1	H_2	H_3	H_4	H_5	
1	15	11	3	–	–	–	–	27
2	13	8	2	1	–	–	–	162
3	12	6	2	–	1	–	–	108
4	11	7	1	2	–	–	–	81
5	10	4	1	1	1	–	–	648
6	9	6	–	3	–	–	–	18
7	9	4	1	–	2	–	–	324
8	$9_{(2)}$	3c	1	1	–	1	–	324
9	9	3	1	–	2	–	–	324
10	9	3p	–	3	–	–	–	18
11	$9_{(3)}$	3c	–	3	–	–	–	108
12	8	3	–	2	1	–	–	648
13	8	2	1	–	1	1	–	648
14	7	3	1	–	–	2	–	27
15	7	2p	–	1	2	–	–	162
16	$7_{(2)}$	2c	–	1	2	–	–	324
17	$7_{(3)}$	2c	–	1	2	–	–	324
18	$7_{[2]}$	1	–	2	–	1	–	162
19	$7_{[1]}$	1	–	1	2	–	–	324
20	7	0	1	–	1	–	1	108
21	7	0	1	–	–	2	–	108
22	6	2c	–	1	1	1	–	648
23	6	2p	–	–	3	–	–	108
24	6	1	–	–	3	–	–	648
25	$6_{[3]}$	0	1	–	–	1	1	216
26	$6_{[2]}$	0	–	2	–	–	1	108
27	$6_{[1]}$	0	–	1	1	1	–	648
28	$6_{[0]}$	0	–	–	3	–	–	36

Segre varieties: (ordinary) Veldkamp lines of $S_{(3)}$)

Tp	Core		Composition					Crd
	Ps	Ls	H_1	H_2	H_3	H_4	H_5	
29	$5_{[1]}$	1	–	1	–	2	–	162
30	$5_{[0]}$	1	–	–	2	1	–	648
31	$5_{(2)}$	0	–	1	1	–	1	324
32	$5_{(1)}$	0	–	1	–	2	–	324
33	$5_{(0)}$	0	–	–	2	1	–	648
34	4	0	–	–	2	–	1	324
35	$4_{(3:1)}$	0	–	–	1	2	–	216
36	$4_{(2:2)}$	0	–	–	1	2	–	324
37	3	1	–	–	–	3	–	54
38	$3_{[1]}$	0	–	1	–	–	2	54
39	$3_{[0]}$	0	–	–	1	1	1	216
40	2	0	–	–	–	2	1	108
41	0	0	–	–	–	–	3	4

Segre varieties: (ordinary) Veldkamp lines of $S_{(3)}$)

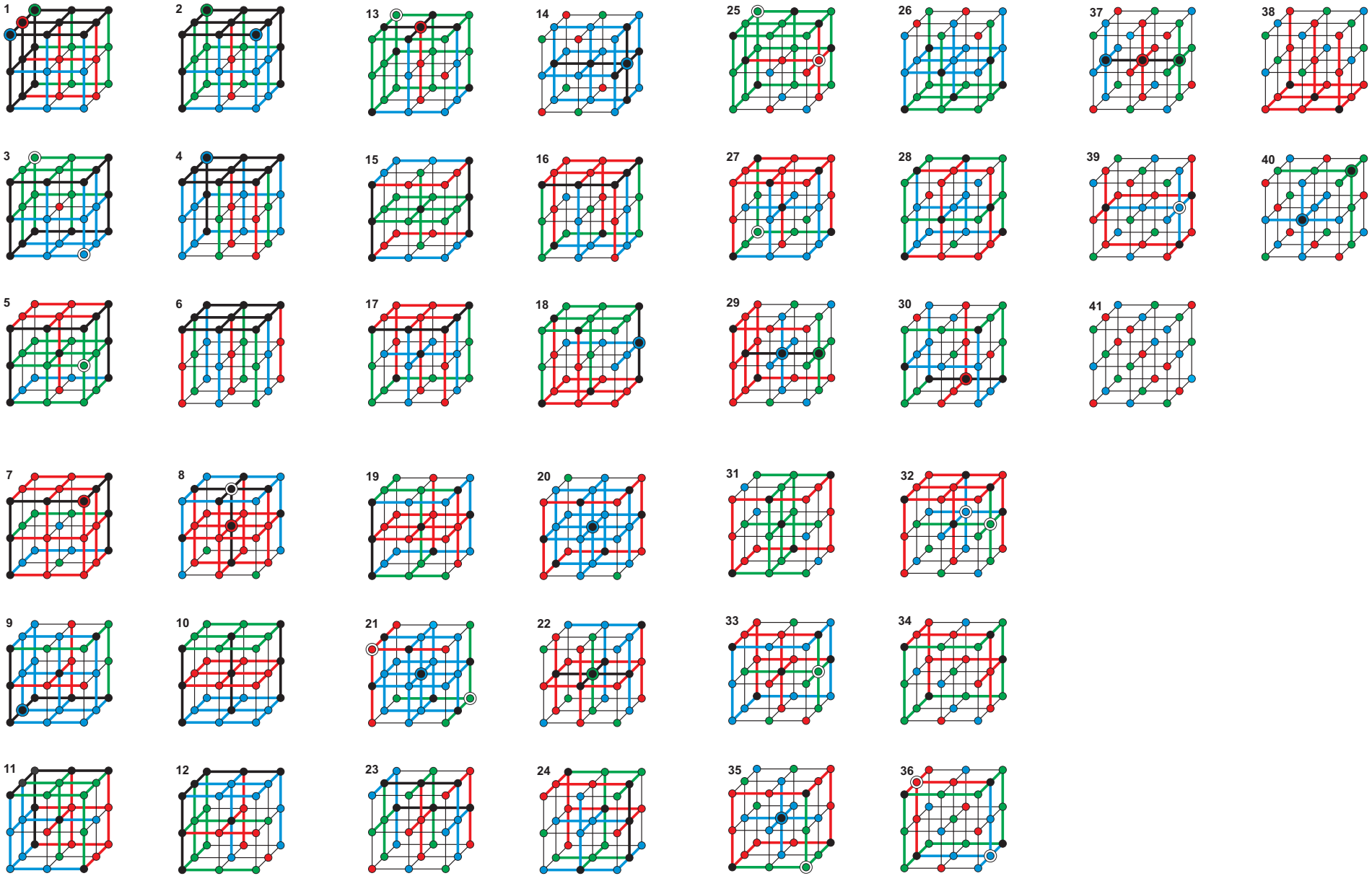

Segre varieties: from $S_{(3)}$ to $S_{(4)}$

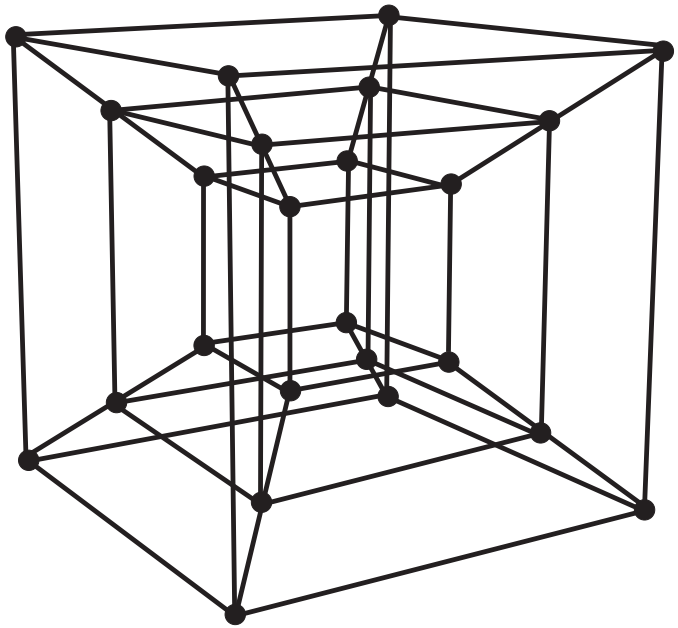

A tesseract-based frame for visualization of the structure of $S_{(4)}$; in order to avoid too crowded appearance of the configuration, there are only shown 24 (out of 81) points and 44 (out of 108) lines.

Segre varieties: geometric hyperplanes of $S_{(4)}$

Tp	Ps	Ls	# of Points of Order					# of $S_{(3)}$'s of Type						VL	Crd	BS	W
			0	1	2	3	4	D	H_1	H_2	H_3	H_4	H_5				
1	65	76	0	0	0	32	33	4	8	0	0	0	0	I	81	2	1
2	57	60	0	0	12	24	21	2	6	4	0	0	0	II, 1	324	3	2
3	53	52	0	2	12	26	13	1	6	3	2	0	0	III, 2	1296	4	2
4	51	48	1	0	12	32	6	0	8	0	4	0	0	3	648	5	2
5	49	44	0	8	12	16	13	1	3	6	0	2	0	IV, 4	648	6	3
6	47	40	0	4	18	20	5	0	4	4	4	0	0	5	3888	11	3
7	45	36	0	18	0	18	9	1	0	9	0	0	2	V, 6	144	7	3
8	45	36	0	0	36	0	9	0	0	12	0	0	0	10	108	17	4
9	45	36	2	4	18	16	5	0	4	2	4	2	0	7, 8	3888	8	3
10	45	36	0	6	18	18	3	0	3	3	6	0	0	9, 11	2592	9	3
11	43	32	1	8	18	12	4	0	2	4	4	2	0	12, 13	7776	12	3
12	41	28	8	0	24	0	9	0	4	0	0	8	0	14	162	14	4
13	41	28	0	12	18	8	3	0	0	6	4	2	0	15, 18	1944	19	4
14	41	28	0	14	12	14	1	0	1	3	6	2	0	17, 21	2592	15	4
15	41	28	2	8	18	12	1	0	1	3	7	0	1	16, 20	2592	10	3
16	41	28	0	8	24	8	1	0	0	4	8	0	0	19	1944	20	4
17	39	24	4	12	12	8	3	0	1	3	3	4	1	22, 25	5184	16	4
18	39	24	3	12	12	12	0	0	0	4	6	0	2	23, 26	1296	22	4
19	39	24	1	12	18	8	0	0	0	2	8	2	0	24, 27	7776	23	4
20	39	24	3	0	36	0	0	0	0	0	12	0	0	28	216	13	3
21	37	20	4	16	12	0	5	0	0	4	0	8	0	29	972	18	4
22	37	20	4	14	12	6	1	0	0	2	5	4	1	30–32	7776	21	4
23	37	20	3	12	18	4	0	0	0	0	8	4	0	33	3888	24	4
24	35	16	4	20	6	4	1	0	0	0	4	8	0	35	1296	28	5
25	35	16	7	12	12	4	0	0	0	0	6	4	2	34, 36	3888	25	4
26	33	12	12	12	6	0	3	0	0	2	0	6	4	37, 38	648	26	5
27	33	12	11	12	6	4	0	0	0	0	4	4	4	39	1296	29	5
28	31	8	13	16	0	0	2	0	0	0	0	8	4	40	648	27	5
29	27	0	27	0	0	0	0	0	0	0	0	0	12	41	24	30	6

Segre varieties: $S_{(4)}$ hyperplanes on a $\mathcal{Q}_0^+(15,2)$

Tp	Ps	Ls	# of Points of Order					# of $S_{(3)}$'s of Type						VL	Crd	BS	W
			0	1	2	3	4	D	H_1	H_2	H_3	H_4	H_5				
1	65	76	0	0	0	32	33	4	8	0	0	0	0	I	81	2	1
2	57	60	0	0	12	24	21	2	6	4	0	0	0	II, 1	324	3	2
3	53	52	0	2	12	26	13	1	6	3	2	0	0	III, 2	1296	4	2
5	49	44	0	8	12	16	13	1	3	6	0	2	0	IV, 4	648	6	3
7	45	36	0	18	0	18	9	1	0	9	0	0	2	V, 6	144	7	3
8	45	36	0	0	36	0	9	0	0	12	0	0	0	10	108	17	4
9	45	36	2	4	18	16	5	0	4	2	4	2	0	7, 8	3888	8	3
10	45	36	0	6	18	18	3	0	3	3	6	0	0	9, 11	2592	9	3
12	41	28	8	0	24	0	9	0	4	0	0	8	0	14	162	14	4
13	41	28	0	12	18	8	3	0	0	6	4	2	0	15, 18	1944	19	4
14	41	28	0	14	12	14	1	0	1	3	6	2	0	17, 21	2592	15	4
15	41	28	2	8	18	12	1	0	1	3	7	0	1	16, 20	2592	10	3
16	41	28	0	8	24	8	1	0	0	4	8	0	0	19	1944	20	4
21	37	20	4	16	12	0	5	0	0	4	0	8	0	29	972	18	4
22	37	20	4	14	12	6	1	0	0	2	5	4	1	30–32	7776	21	4
23	37	20	3	12	18	4	0	0	0	0	8	4	0	33	3888	24	4
26	33	12	12	12	6	0	3	0	0	2	0	6	4	37, 38	648	26	5
27	33	12	11	12	6	4	0	0	0	0	4	4	4	39	1296	29	5

The types of geometric hyperplanes of $S_{(4)}$ lying on the unique hyperbolic quadric $\mathcal{Q}_0^+(15,2) \subset PG(15,2)$ that contains the $S_{(4)}$ (the first orbit) and is invariant under its stabilizer group; these are precisely hyperplane types that originate from those types of (ordinary) Veldkamp lines of $S_{(3)}$ whose cores feature *odd* number of points.

Segre varieties: six particular h-types on the $\mathcal{Q}_0^+(15,2)$

Tp	Ps	Ls	# of Points of Order					# of $S_{(3)}$'s of Type						VL	Crd	BS	W
			0	1	2	3	4	D	H_1	H_2	H_3	H_4	H_5				
1	65	76	0	0	0	32	33	4	8	0	0	0	0	I	81	2	1
2	57	60	0	0	12	24	21	2	6	4	0	0	0	II, 1	324	3	2
5	49	44	0	8	12	16	13	1	3	6	0	2	0	IV, 4	648	6	3
8	45	36	0	0	36	0	9	0	0	12	0	0	0	10	108	17	4
12	41	28	8	0	24	0	9	0	4	0	0	8	0	14	162	14	4
21	37	20	4	16	12	0	5	0	0	4	0	8	0	29	972	18	4

Six types of hyperplanes lying on $\mathcal{Q}_0^+(15,2)$ that in their totality correspond to the image of the set of 2295 maximal subspaces of the symplectic polar space $\mathcal{W}(7,2)$. Interestingly, one orbit consists of homogeneous hyperplanes, viz. of those whose all $S_{(3)}$'s are of type H_2; note that they are exactly the types whose members feature no $S_{(3)}$ of type H_3 and H_5, each of them also exhibiting points of maximum order.

...Cayley-Dickson algebras

Cayley-Dickson Algebras and Finite Geometry

Cayley-Dickson algebras represent a nested sequence $A_0, A_1, A_2, \ldots, A_N, \ldots$ of 2^N-dimensional (in general non-associative) $\mathbb{R}$-algebras with $A_N \subset A_{N+1}$, where $A_0 = \mathbb{R}$ and where for any $N \geq 0$ A_{N+1} comprises all ordered pairs of elements from A_N with conjugation defined by

$$(x, y)^* = (x^*, -y) \tag{4}$$

and multiplication usually by

$$(x, y)(X, Y) = (xX - Yy^*, x^*Y + Xy). \tag{5}$$

Cayley-Dickson Algebras and Finite Geometry

Every finite-dimensional algebra is basically defined by the multiplication rule of its basis.
The basis elements (or units) $e_0, e_1, e_2, \ldots, e_{2^{N+1}-1}$ of A_{N+1}, e_0 being the real basis element (identity), can be chosen in various ways.
Our preference is the *canonical* basis

$$\begin{array}{llllll} e_0 = (e_0, 0), & e_1 = (e_1, 0), & e_2 = (e_2, 0), & \ldots, & e_{2^N-1} & = (e_{2^N-1}, 0), \\ e_{2^N} = (0, e_0), & e_{2^N+1} = (0, e_1), & e_{2^N+2} = (0, e_2), & \ldots, & e_{2^{N+1}-1} & = (0, e_{2^N-1}), \end{array}$$

where, by abuse of notation, the same symbols are also used for the basis elements of A_N.
This is because one focuses on *multiplication* properties of basis elements and the canonical basis seems to display most naturally the inherent symmetry of this operation.
For, in addition to revealing the nature of the Cayley-Dickson recursive process, it also implies that for both a and b being non-zero we have $e_a e_b = \pm e_{a \oplus b}$, where the symbol '$\oplus$' denotes '*exclusive or*' of the binary representations of a and b.

Cayley-Dickson Algebras and Finite Geometry

Employing a multiplication table of A_N, $N \geq 2$, it can be verified that the $2^N - 1$ imaginaries e_a, $1 \leq a \leq 2^N - 1$, form $\binom{2^N-1}{2}/3$ distinguished sets each of which comprises three different units $\{e_a, e_b, e_c\}$ that satisfy equation

$$e_a e_b = \pm e_c, \tag{6}$$

and where each unit is found to belong to $2^{N-1} - 1$ such sets.

Regarding the imaginaries as points and their distinguished triples as lines, one gets a point-line incidence geometry where every line has three points and through each point there pass $2^{N-1} - 1$ lines and which is isomorphic to PG$(N - 1, 2)$.

Cayley-Dickson Algebras and Finite Geometry

Let us assume, without loss of generality, that the elements in any distinguished triple $\{e_a, e_b, e_c\}$ of A_N are ordered in such a way that $a < b < c$.

Then, for $N \geq 3$, we can naturally speak about two different kinds of triples and, hence, two distinct kinds of lines of the associated 2^N-nionic PG$(N-1, 2)$, according as $a + b = c$ or $a + b \neq c$; in what follows a line of the former/latter kind will be called ordinary/defective.

This stratification of the line-set of the PG$(N-1, 2)$ induces a similar partition of the point-set of the latter space into several types, where a point of a given type is characterized by the same number of lines of either kind that pass through it.

Cayley-Dickson Algebras and ... Veldkamp Spaces

Obviously, if our projective space PG$(N-1,2)$ is regarded as an *abstract* geometry *per se*, every point and/or every line in it has the same footing.

So, to account for the above-described 'refinement' of the structure of our 2^N-nionic PG$(N-1,2)$, it turns out to be necessary to find a representation of this space where each point/line is ascribed a certain 'internal' structure.

Such a representation is naturally provided by Veldkamp spaces!

Octonions and the Pasch $(6_2, 4_3)$-configuration

$*$	1	2	3	4	5	6	7
1	-0	-3	$+2$	-5	$+4$	$+7$	-6
2	$+3$	-0	-1	-6	-7	$+4$	$+5$
3	-2	$+1$	-0	-7	$+6$	-5	$+4$
4	$+5$	$+6$	$+7$	-0	-1	-2	-3
5	-4	$+7$	-6	$+1$	-0	$+3$	-2
6	-7	-4	$+5$	$+2$	-3	-0	$+1$
7	$+6$	-5	-4	$+3$	$+2$	-1	-0

The multiplication table of the imaginary unit octonions e_a, $1 \leq a \leq 7$. For the sake of simplicity, in what follows we shall employ a short-hand notation $e_a \equiv a$; likewise for the real unit $e_0 \equiv 0$. There are also delineated multiplication tables corresponding to the distinguished nested sequence of sub-algebras of complex numbers ($a = 1$, the upper left corner) and quaternions ($1 \leq a \leq 3$, the upper left 3×3 square).

Octonions and the Pasch $(6_2, 4_3)$-configuration

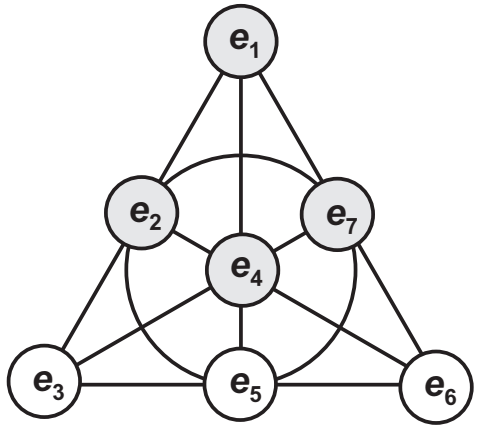

PG(2, 2), the Fano plane, that provides the multiplication law for octonions.
We have six ordinary lines,

$$\{1,2,3\},\{1,4,5\},\{1,6,7\},\{2,4,6\},\{2,5,7\},\{3,4,7\},$$

and only single defective one,

$$\{3,5,6\}.$$

Similarly, our octonionic PG(2, 2) features two distinct types of points. A type-one point is such that two lines passing through it are ordinary, the remaining one being defective; such a point lies in the set

$$\{3,5,6\} \equiv \alpha.$$

A type-two point is such that every line passing through it is ordinary; such a point belongs to the set

$$\{1,2,4,7\} \equiv \beta,$$

which is highlighted by gray color in the figure.

Octonions and the Pasch $(6_2, 4_3)$-configuration

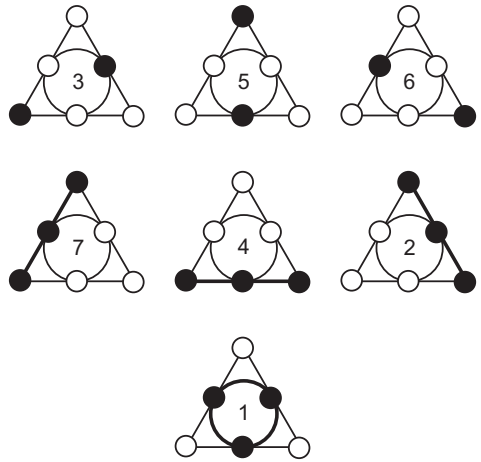

The seven geometric hyperplanes of the Pasch configuration.

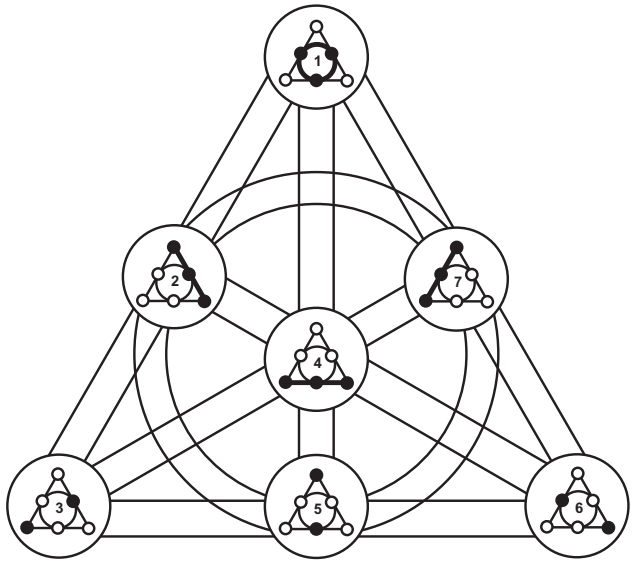

A unified view of the seven Veldkamp lines of the Pasch configuration.

Sedenions and the Desargues (10_3)-configuration

$*$	1	2	3	4	5	6	7	8	9	10	11	12	13	14	15
1	-0	-3	$+2$	-5	$+4$	$+7$	-6	-9	$+8$	$+11$	-10	$+13$	-12	-15	$+14$
2	$+3$	-0	-1	-6	-7	$+4$	$+5$	-10	-11	$+8$	$+9$	$+14$	$+15$	-12	-13
3	-2	$+1$	-0	-7	$+6$	-5	$+4$	-11	$+10$	-9	$+8$	$+15$	-14	$+13$	-12
4	$+5$	$+6$	$+7$	-0	-1	-2	-3	-12	-13	-14	-15	$+8$	$+9$	$+10$	$+11$
5	-4	$+7$	-6	$+1$	-0	$+3$	-2	-13	$+12$	-15	$+14$	-9	$+8$	-11	$+10$
6	-7	-4	$+5$	$+2$	-3	-0	$+1$	-14	$+15$	$+12$	-13	-10	$+11$	$+8$	-9
7	$+6$	-5	-4	$+3$	$+2$	-1	-0	-15	-14	$+13$	$+12$	-11	-10	$+9$	$+8$
8	$+9$	$+10$	$+11$	$+12$	$+13$	$+14$	$+15$	-0	-1	-2	-3	-4	-5	-6	-7
9	-8	$+11$	-10	$+13$	-12	-15	$+14$	$+1$	-0	$+3$	-2	$+5$	-4	-7	$+6$
10	-11	-8	$+9$	$+14$	$+15$	-12	-13	$+2$	-3	-0	$+1$	$+6$	$+7$	-4	-5
11	$+10$	-9	-8	$+15$	-14	$+13$	-12	$+3$	$+2$	-1	-0	$+7$	-6	$+5$	-4
12	-13	-14	-15	-8	$+9$	$+10$	$+11$	$+4$	-5	-6	-7	-0	$+1$	$+2$	$+3$
13	$+12$	-15	$+14$	-9	-8	-11	$+10$	$+5$	$+4$	-7	$+6$	-1	-0	-3	$+2$
14	$+15$	$+12$	-13	-10	$+11$	-8	-9	$+6$	$+7$	$+4$	-5	-2	$+3$	-0	-1
15	-14	$+13$	$+12$	-11	-10	$+9$	-8	$+7$	-6	$+5$	$+4$	-3	-2	$+1$	-0

The multiplication table of the imaginary unit sedenions e_a, $1 \leq a \leq 15$. As in the previous section, we shall employ a short-hand notation $e_a \equiv a$; likewise for the real unit $e_0 \equiv 0$. There are also shown multiplication tables corresponding to the distinguished nested sequence of sub-algebras starting with complex numbers ($a = 1$), quaternions ($1 \leq a \leq 3$) and octonions ($1 \leq a \leq 7$).

Sedenions and the Desargues (10_3)-configuration

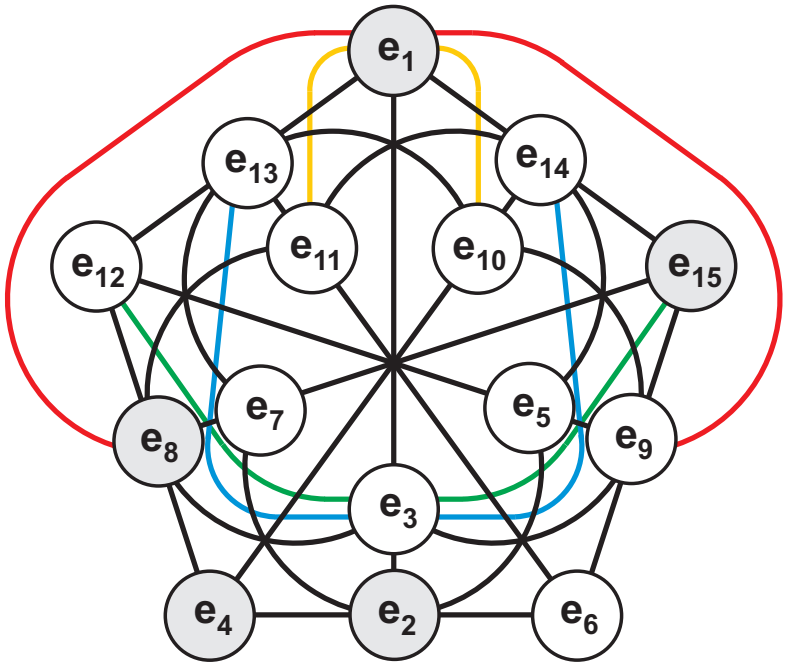

An illustration of the structure of PG(3, 2) that provides the multiplication law for sedenions. As in the previous case, the three imaginaries lying on the same line are such that the product of two of them yields the third one, sign disregarded.

We have here 25 ordinary and 10 defective lines, and two distinct kinds of points.

Sedenions and the Desargues (10_3)-configuration

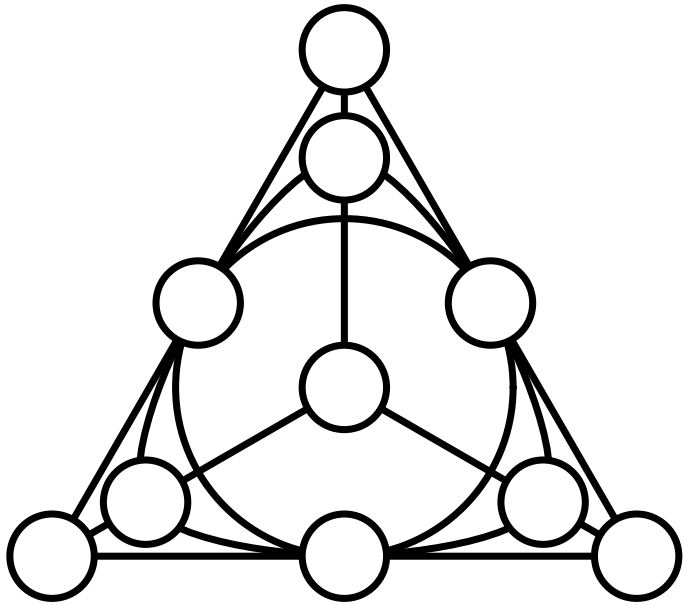

An illustrative portrayal of the Desargues configuration, built around the model of the Pasch configuration: circles stand for its points, whereas its lines are represented by triples of points on common straight segments (six), arcs of circles (three) and a big circle.

Sedenions and the Desargues (10_3)-configuration

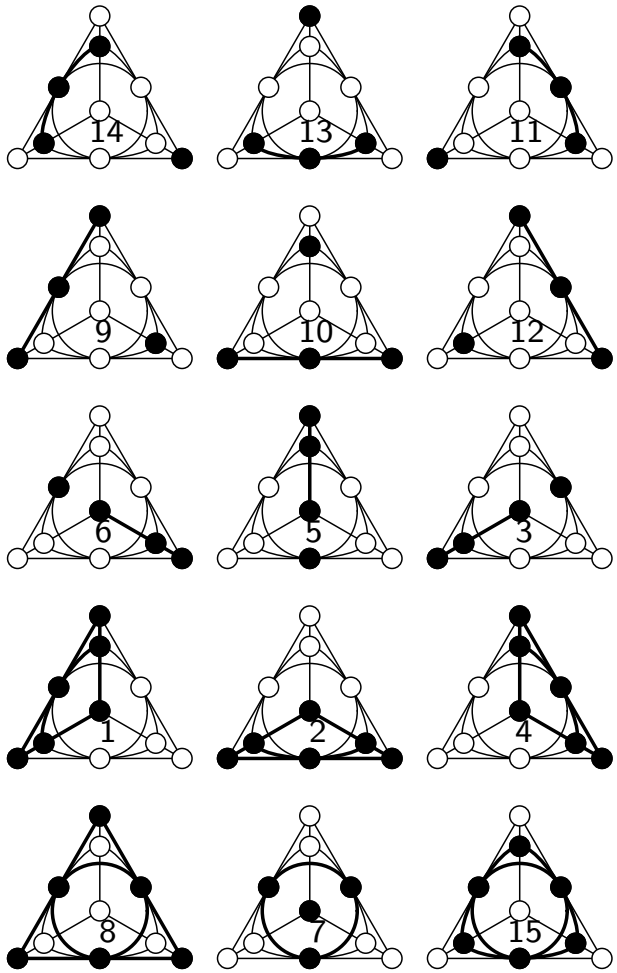

The fifteen geometric hyperplanes of the Desargues configuration. The hyperplanes are labelled by imaginary units of sedenions in such a way that the 35 lines of the Veldkamp space of the Desargues configuration are identical with the 35 distinguished triples of units.

Sedenions and the Desargues (10_3)-configuration

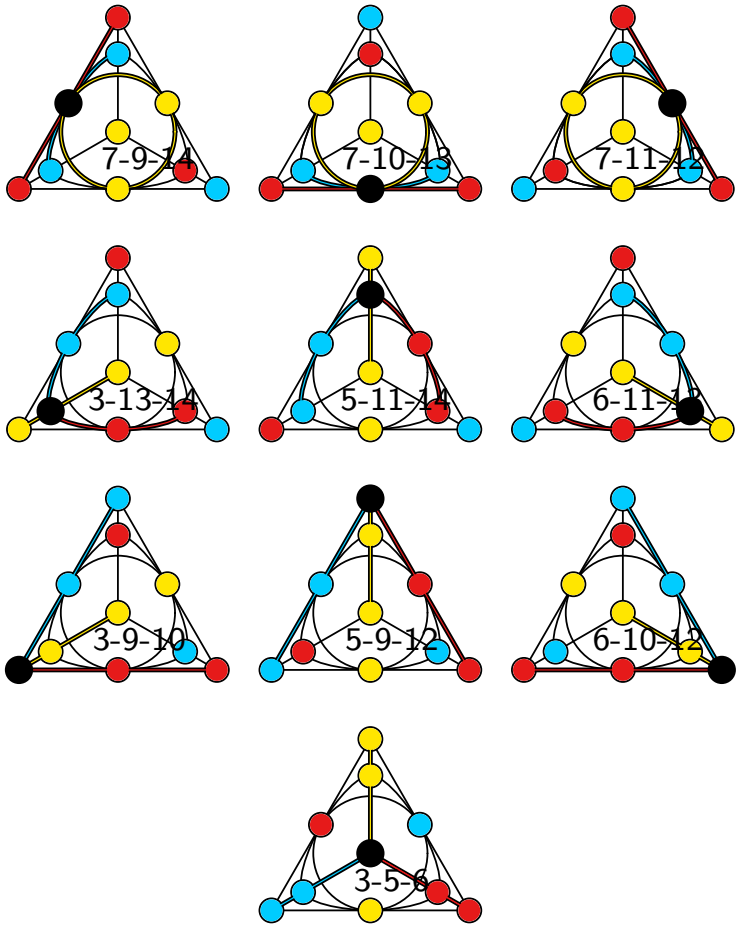

The ten Veldkamp lines of the Desargues configuration that represent the ten *defective* lines of the sedenionic PG(3, 2). The three geometric hyperplanes comprising a given Veldkamp line are distinguished by different colors, with their common elements (here just a single point) being colored black. For each Veldkamp line we also explicitly indicate its composition.

Sedenions and the Desargues (10_3)-configuration

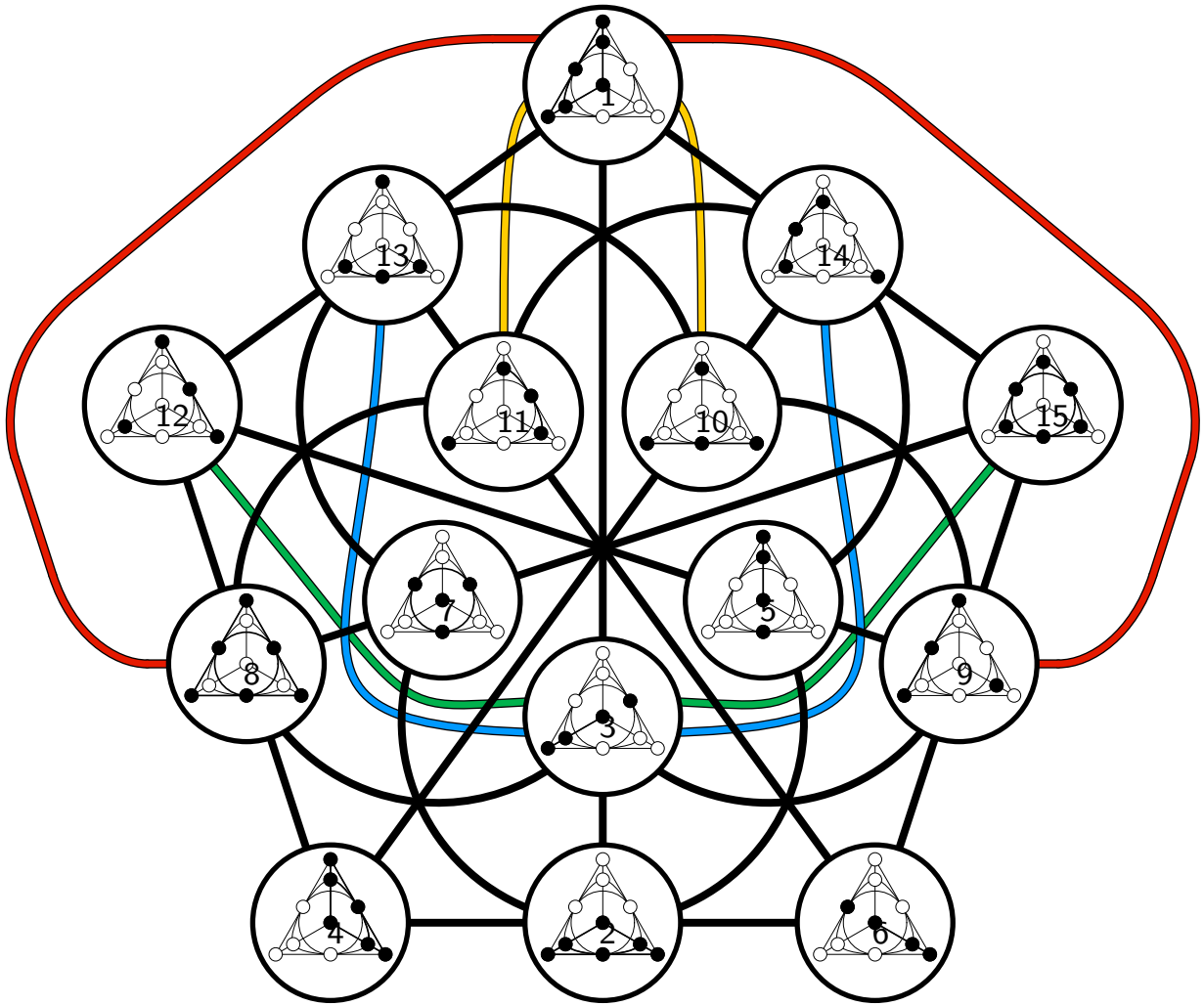

A compact graphical view of illustrating the bijection between 15 imaginary unit sedenions and 15 geometric hyperplanes of the Desargues configuration, as well as between 35 distinguished triples of units and 35 Veldkamp lines of the Desargues configuration.

32-nions and the Cayley-Salmon $(15_4, 20_3)$-configuration

The 155 lines of the associated PG(4, 2) split into

- 65 defective and
- 90 ordinary.

However, unlike the preceding two cases, there are *three* different types of points in our 32-nionic PG(4, 2):

- 10 α-points, each of which is on nine defective and six ordinary lines;
- 15 β-points, each of which is on seven defective and eight ordinary lines; and
- 6 γ-points, each of them being on fifteen ordinary (and, hence, on zero defective) lines.

This stratification of the point-set of PG(4, 2) leads, in turn, to two different kinds of defective lines and three distinct kinds of ordinary lines.

32-nions and the Cayley-Salmon $(15_4, 20_3)$-configuration

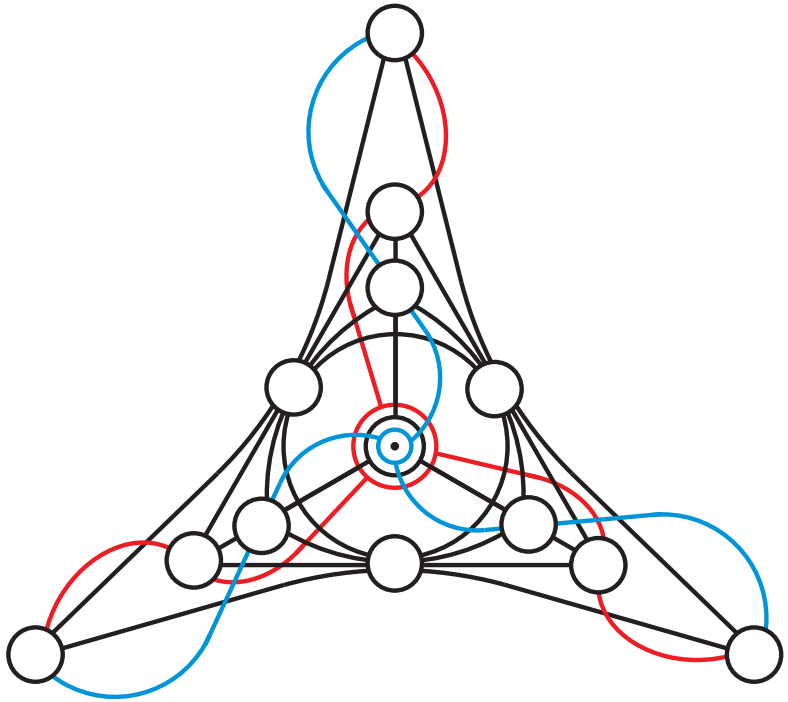

An illustration of the structure of the $(15_4, 20_3)$-configuration, built around the model of the Desargues configuration. The five points added to the Desargues configuration are the three peripheral points and the red and blue point in the center. The ten lines added are three lines denoted by red color, three blue lines, three lines joining pairwise the three peripheral points and the line that comprises the three points in the center of the figure, that is the ones represented by a bigger red circle, a smaller blue circle and a medium-sized black one.

32-nions and the Cayley-Salmon $(15_4, 20_3)$-configuration

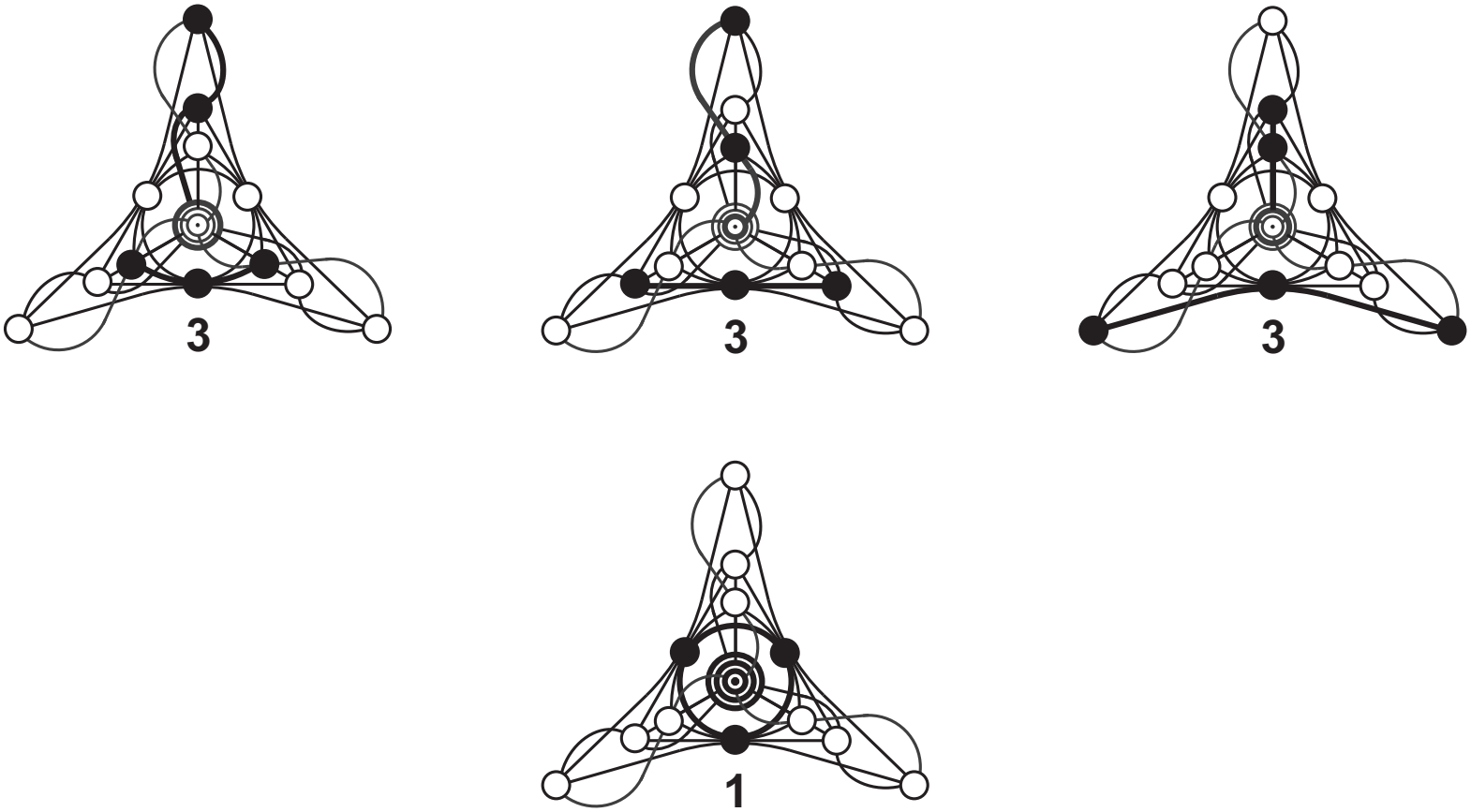

The ten geometric hyperplanes of the $(15_4, 20_3)$-configuration of type one; the number below a subfigure indicates how many hyperplane's copies we get by rotating the particular subfigure through 120 degrees around its center.

32-nions and the Cayley-Salmon $(15_4, 20_3)$-configuration

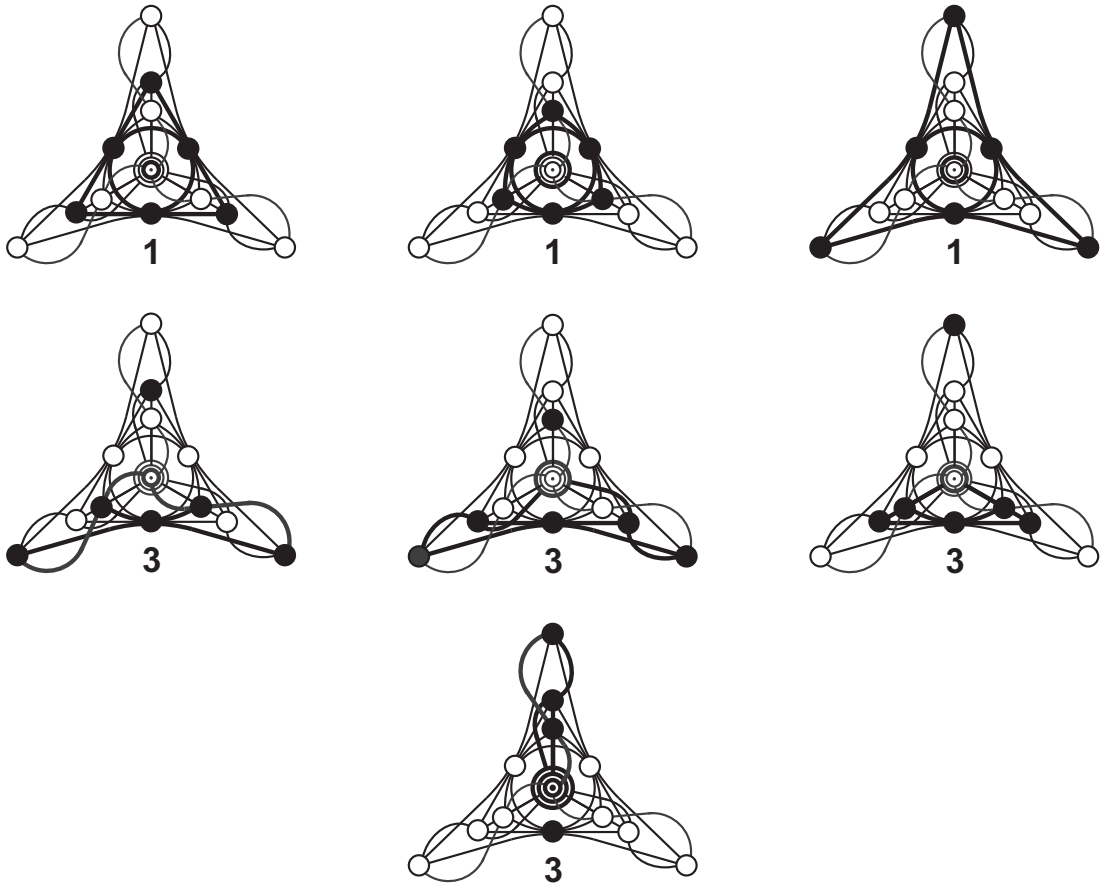

The fifteen geometric hyperplanes of the $(15_4, 20_3)$-configuration of type two.

32-nions and the Cayley-Salmon $(15_4, 20_3)$-configuration

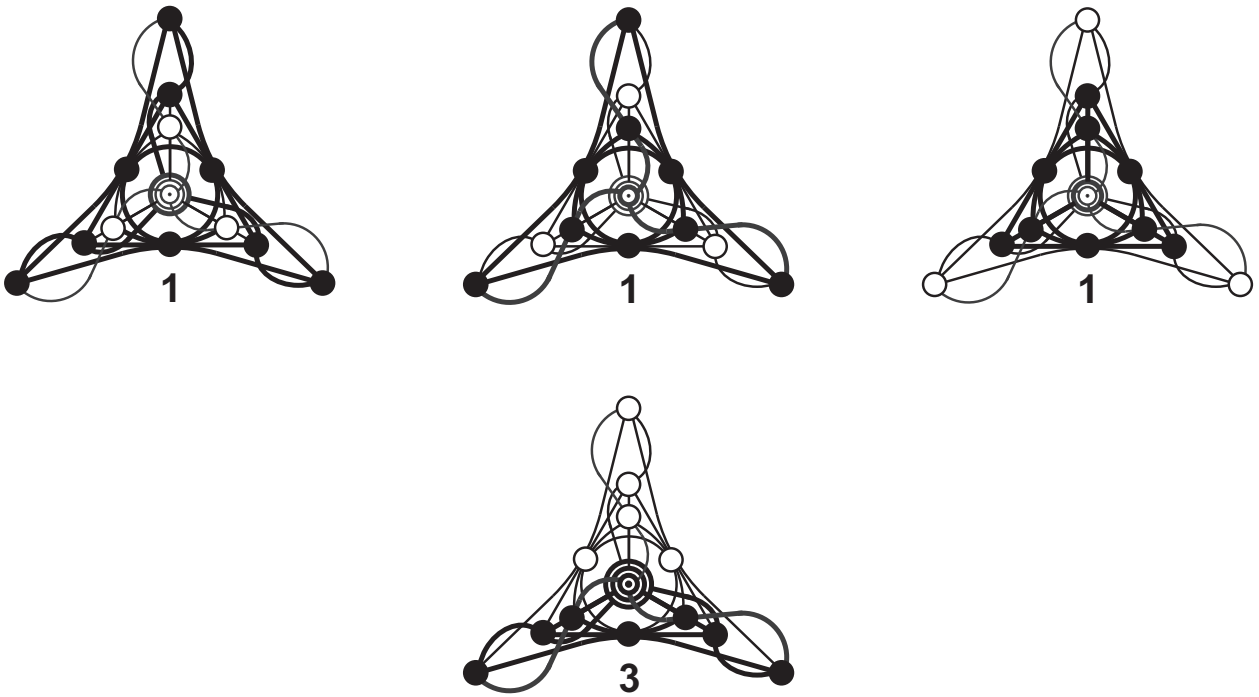

The six geometric hyperplanes of the $(15_4, 20_3)$-configuration of type three.

32-nions and the Cayley-Salmon $(15_4, 20_3)$-configuration

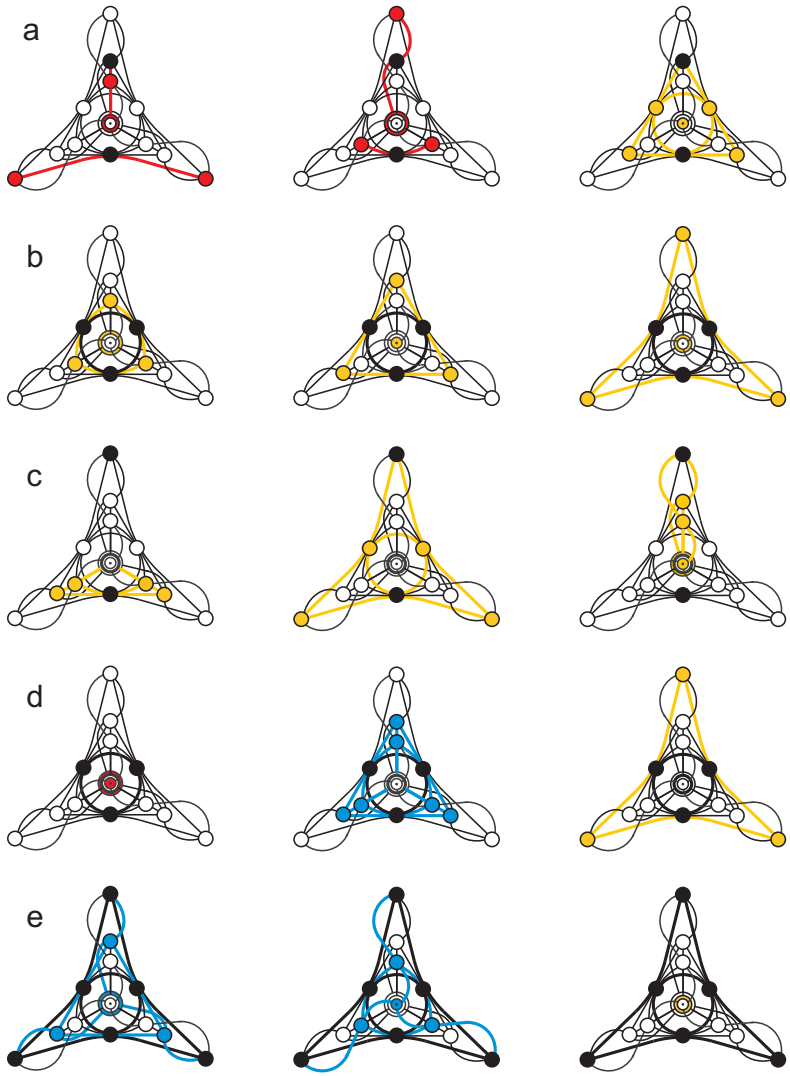

The five types of Veldkamp lines of the $(15_4, 20_3)$-configuration. Here, each representative of a geometric hyperplane is drawn separately and different colors are used to distinguish between different hyperplane types: red is reserved for type one, yellow for type two and blue for type three hyperplanes.

Cayley-Salmon $(15_4, 20_3)$-configuration

Cayley-Salmon configuration lives in

- PG(3, 2) (as the line-complement of a GQ(2, 2)),
- in the so-called *Hexagrammum Mysticum* of Pascal (15 Salmon points and 20 Cayley lines).

Three distinct views of Cayley-Salmon configuration:

- One is as three pairwise-disjoint triangles that are in perspective from a line, in which case the centers of perspectivity are guaranteed by Desargues' theorem to also lie on a line; these two lines form a geometric hyperplane of type one;
- The other view of the figure takes any point of the configuration to be the center of perspectivity of two quadrangles whose six pairs of corresponding sides meet necessarily in the points of a Pasch configuration; the point and the associated Pasch configuration form a geometric hyperplane of type two;
- The incidence sum of a Desargues configuration and three triangles on a commmon side.

2^N-nions and a $\left(\binom{N+1}{2}_{N-1}, \binom{N+1}{3}_3\right)$-configuration

If one also includes the trivial cases of complex numbers ($N = 1$), where the relevant geometry is just a single point i. e. the $(1_0, 0_3)$-configuration, and quaternions ($N = 2$), whose geometry is a single line i. e. the $(3_1, 1_3)$-configuration, we obtain the following nested sequence of configurations whose Veldkamp spaces capture the stratification/partition of the point- and line-sets of the 2^N-nionic PG$(N-1, 2)$, N being a positive integer,

$$(1_0, 0_3),$$

$$(3_1, 1_3),$$

$$(6_2, 4_3),$$

$$(10_3, 10_3),$$

$$(15_4, 20_3),$$

$$(21_5, 35_3),$$

$$\ldots,$$

$$\left(\binom{N+1}{2}_{N-1}, \binom{N+1}{3}_3\right),$$

$$\ldots.$$

2^N-nions and a $\left(\binom{N+1}{2}_{N-1}, \binom{N+1}{3}_3\right)$-configuration

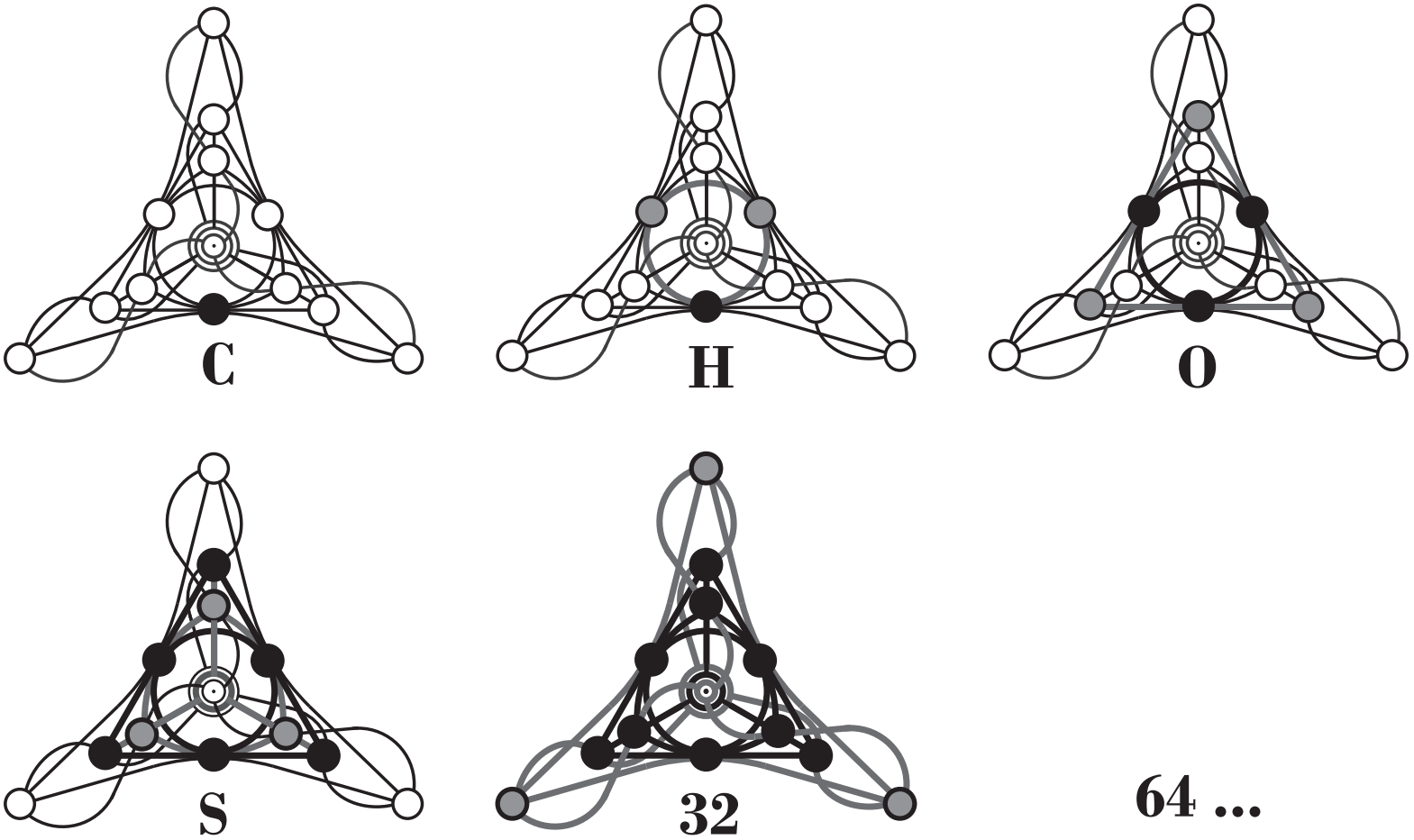

Figure: A nested hierarchy of finite $\left(\binom{N+1}{2}_{N-1}, \binom{N+1}{3}_3\right)$-configurations of 2^N-nions for $1 \leq N \leq 5$ when embedded in the Cayley-Salmon configuration ($N = 5$).

2^N-nions and combinatorial grassmannians

A combinatorial Grassmannian $G_k(|X|)$, where k is a positive integer and X is a finite set, is a point-line incidence structure whose points are k-element subsets of X and whose lines are $(k+1)$-element subsets of X, incidence being inclusion.

If $|X| = N+1$ and $k = 2$, $G_2(N+1)$ is nothing but our binomial $\left(\binom{N+1}{2}_{N-1}, \binom{N+1}{3}_3\right)$-configuration.

2^N-nions and combinatorial grassmannians

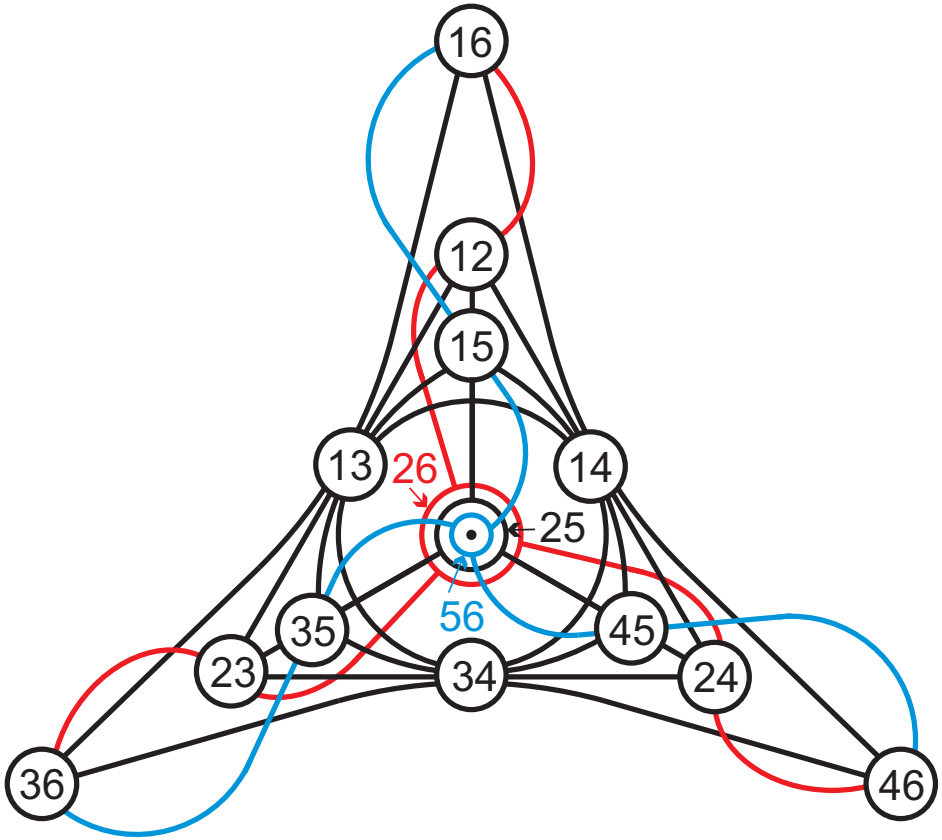

A diagrammatical proof of the isomorphism between $\mathcal{C}_5$ and $G_2(6)$. The points of $\mathcal{C}_5$ are labeled by pairs of elements from the set $\{1, 2, \ldots, 6\}$ in such a way that each line of the configuration is indeed of the form $\{\{a, b\}, \{a, c\}, \{b, c\}\}$, $a \neq b \neq c \neq a$.

Slight digression: labeled Fano planes and...

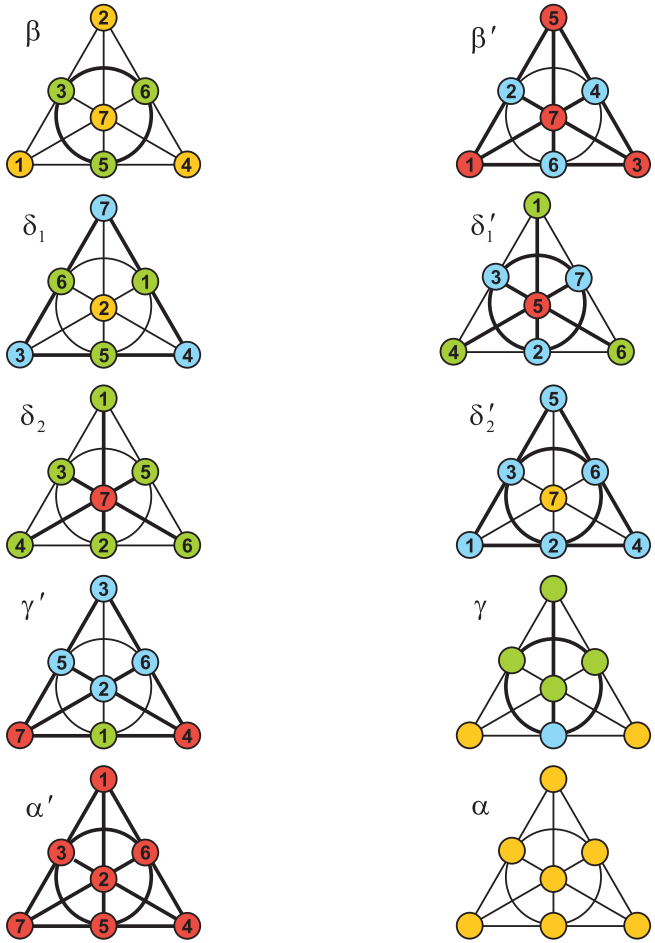

A Fano plane can be labeled by integers from 1 to 7 in 30 different ways, which fall into eight distinct types shown above. (Here, a defective line is drawn bold and a point colored red, blue, green or yellow is of order three, two, one or zero, respectively; the order of a point is the number of defective lines passing through it.)

Slight digression: ...their Veldkamp spaces

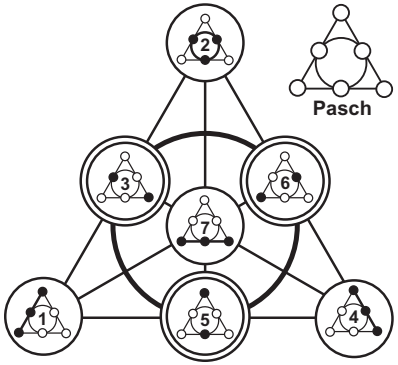

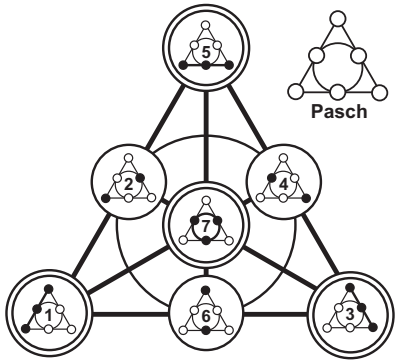

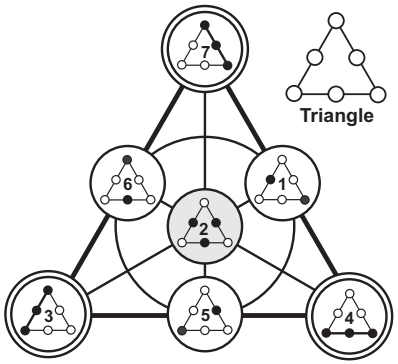

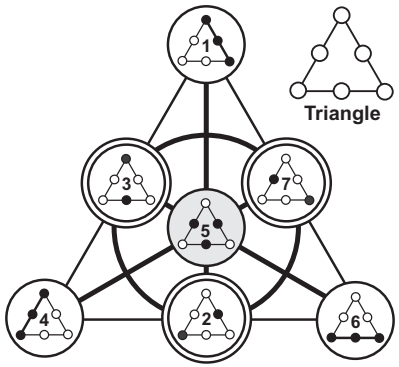

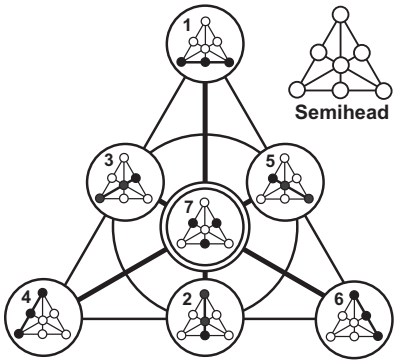

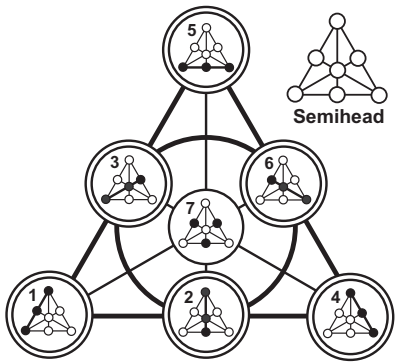

Slight digression: ...their Veldkamp spaces

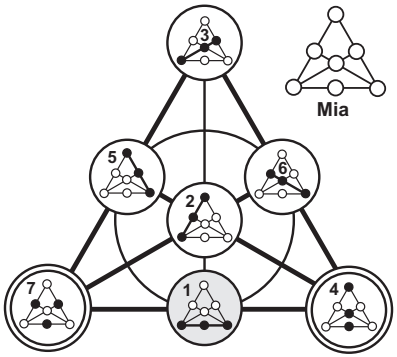

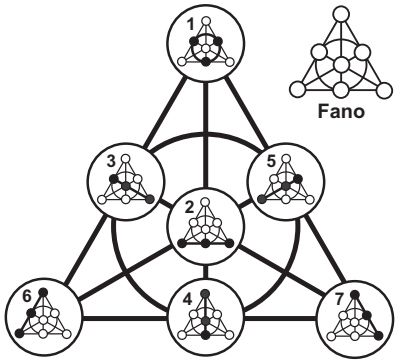

...Dynkin diagrams

Dynkin diagrams

Dynkin diagrams were introduced in the theory of Lie groups/algebras to describe particular sets of elements in lattices possessing integer quadratic forms – so-called root systems. Given a root systems and its basis S, the vertices/nodes of its Dynkin diagram are the roots of S and two nodes are not connected if the corresponding roots are orthogonal.

In addition, a Dynkin diagram also encodes the lengths of roots. That is done by marking the edge connecting two vertices whose corresponding roots are of different length with an arrow pointing to the shorter root.

Given a simple Lie algebra with its highest root γ, an extended root system is obtained by adding $-\gamma$ to the set of simple roots, which leads to the notion the *extended* Dynkin diagram of the algebra in question. We will only be dealing with a particularly simple type of extended Dynkin diagrams, namely $\widetilde{D}_n$ $(4 \leq n)$, depicted in the next figure.

$\widetilde{D}_n$

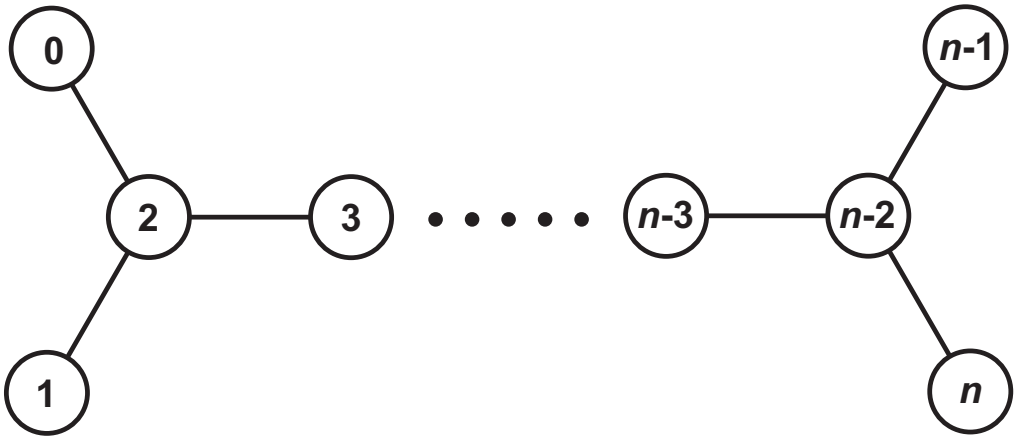

An illustration of the extended Dynkin diagram of type $\widetilde{D}_n$, $4 \leq n$, with its vertices labeled by integers from 0 to n.

Veldkamp Spaces of $\widetilde{D}_n$ and Two-Qubit Pauli Group

$\widetilde{D}_n$, like any other graph, can be viewed/interpreted as a particular point-line incidence structure, $\mathcal{C}(\widetilde{D}_n)$, whose points and lines are, respectively, vertices and edges of $\widetilde{D}_n$; it thus features $n+1$ points and n lines, where, for $5 \leq n$, four points are of order one, two of order three and the remaining $n-5$ points being of order two.

Let us adopt this view and have a detailed look at properties of the Veldkamp space of $\mathcal{C}(\widetilde{D}_n)$.

We shall carry out this task step by step for $4 \leq n \leq 8$ in order to see how naturally the two-qubit (and, at the end, also three-qubit) Pauli group enters the stage.

Case $n = 4$: geometric hyperplanes

$\mathcal{C}(\widetilde{D}_4)$ features altogether 16 different geometric hyperplanes as listed below and portrayed in the next figure.

We see that each hyperplane except for the last one contains point '2'; moreover, H_{15} consists solely of this particular point and is thus contained in all preceding 14 hyperplanes. We further note that any other point of $\mathcal{C}(\widetilde{D}_4)$ is located in eight hyperplanes.

	H_1	H_2	H_3	H_4	H_5	H_6	H_7	H_8	H_9	H_{10}	H_{11}	H_{12}	H_{13}	H_{14}	H_{15}	H_{16}
0	+					+	+	+	+	+	+					+
1		+			+		+	+			+		+	+		+
2	+	+	+	+	+	+	+	+	+	+	+	+	+	+	+	
3				+	+	+	+		+			+	+			+
4			+		+	+		+		+		+		+		+

The composition of 16 geometric hyperplanes H_i, $1 \leq i \leq 16$, of $\mathcal{C}(\widetilde{D}_4)$. The '+' symbol indicates which point of $\mathcal{C}(\widetilde{D}_4)$ lies in a given hyperplane.

Case $n = 4$: geometric hyperplanes

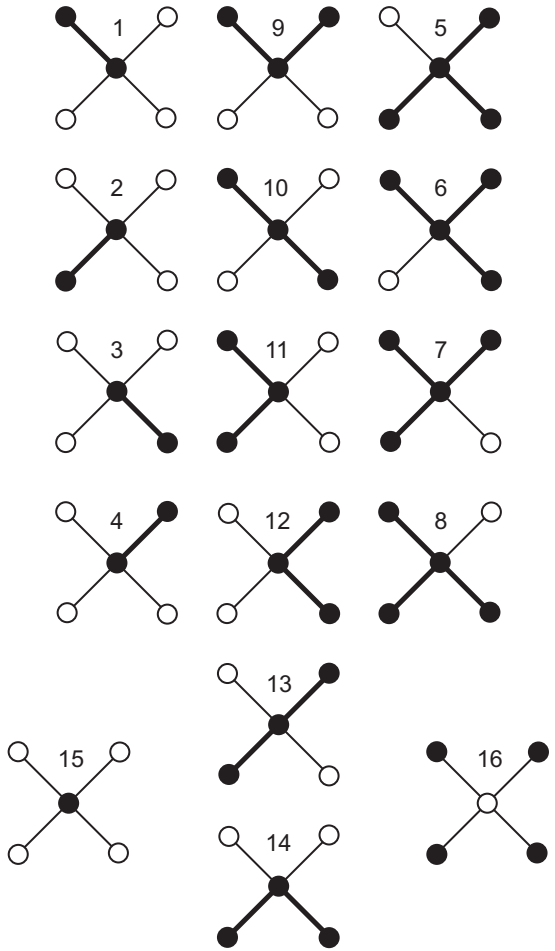

A diagrammatical representation of geometric hyperplanes of $\mathcal{C}(\widetilde{D}_4)$. Here, and in the sequel, a point of a hyperplane is represented by a filled circle and a line is drawn heavy if both of its points lie in the hyperplane.

Case $n = 4$: 35 three-point Veldkamp lines

	H_1	H_2	H_3	H_4	H_5	H_6	H_7	H_8	H_9	H_{10}	H_{11}	H_{12}	H_{13}	H_{14}	H_{15}	H_{16}
1	+	+										+				
2	+		+										+			
3	+			+										+		
4	+				+										+	
5	+					+					+					
6	+						+			+						
7	+							+	+							
8		+	+						+							
9		+		+						+						
10		+			+						+					
11		+				+									+	
12		+					+							+		
13		+						+					+			
14			+	+							+					
15			+		+					+						
16			+			+								+		
17			+				+								+	
18			+					+				+				
19				+	+				+							
20				+		+							+			
21				+			+					+				
22				+				+							+	
23					+	+						+				
24					+		+						+			
25					+			+						+		
26						+	+		+							
27						+		+		+						
28							+	+			+					
29									+	+	+					
30									+			+	+			
31									+					+	+	
32										+		+		+		
33										+			+		+	
34											+	+			+	
35											+		+	+		

Case $n = 4$: PG$(3, 2)$ and two-qubit Pauli group

One sees that no such Veldkamp line contains H_{16}, the latter being thus regarded as an exceptional Veldkamp point of the geometry; the remaining 15 hyperplanes and all 35 Veldkamp lines form the projective space PG$(3, 2)$.

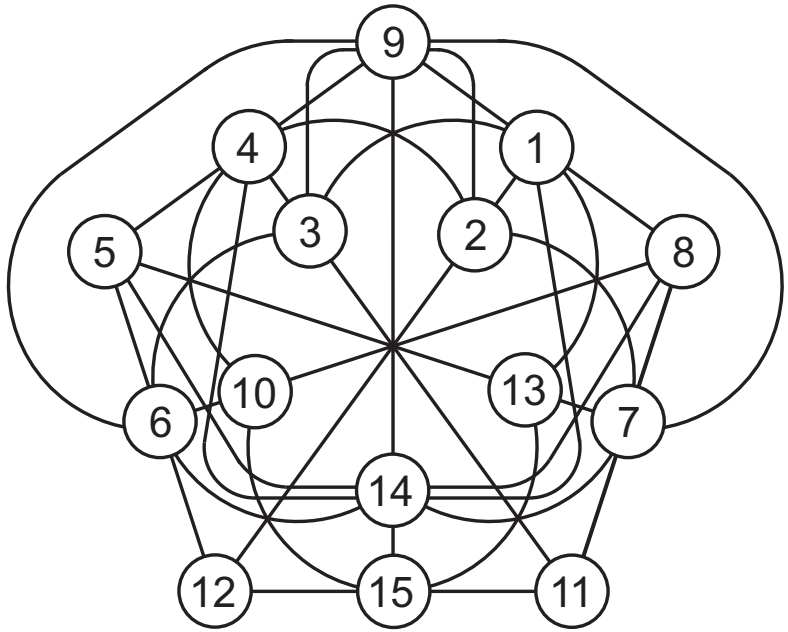

Case $n = 4$: PG$(3, 2)$ and two-qubit Pauli group

Let us now return back to our $\widetilde{D}_4$ and label its five vertices by five distinct elements of the two-qubit Pauli group, $\overline{\mathcal{P}}_2$.

One can take any five elements requiring only that their product equals II; this constraint is necessary to ensure that the induced labeling of the points the associated Veldkamp space has the property that the product of any three collinear elements is also equal to II.

Given the symmetry of $\widetilde{D}_4$, one of the most natural choices is ($A \otimes B$ is shorthanded to AB in the sequel)

$$0 \to XI,\ 1 \to IX,\ 2 \to YY,\ 3 \to ZI,\ 4 \to IZ.$$

Case $n = 4$: PG(3, 2) and two-qubit Pauli group

Assume further that each hyperplane acquires the label that is the product of the group elements attached to the points it consists of; thus, for example, H_1, comprising points 0 and 2, will bear the label $(XI).(YY) = ZY$.

Hence, we arrive at a particular *one-to-one* correspondence between the 15 Veldkamp points of $\mathcal{C}(\widetilde{D}_4)$ and the 15 elements of $\overline{\mathcal{P}}_2$: note that the 'exceptional' hyperplane H_{16} corresponds to the same group element as H_{15}, because the two hyperlanes are complementary.

$\mathcal{C}(\widetilde{D}_4)$	H_1	H_2	H_3	H_4	H_5	H_6	H_7	H_8	H_9	H_{10}	H_{11}	H_{12}	H_{13}	H_{14}	H_{15}	H_{16}
$\overline{\mathcal{P}}_2$	ZY	YZ	YX	XY	XI	IX	IZ	ZI	IY	ZX	ZZ	XX	XZ	YI	YY	YY

Case $n = 4$: PG$(3, 2)$ and two-qubit Pauli group

It is easy to check that not only is the product of three elements on each Veldkamp line equal to the identity element of the group, but – as handy rendered by the figure below – the three elements that lie on a line of the selected copy of $W(3, 2)$ our PG$(3, 2)$ was built around pairwise commute.

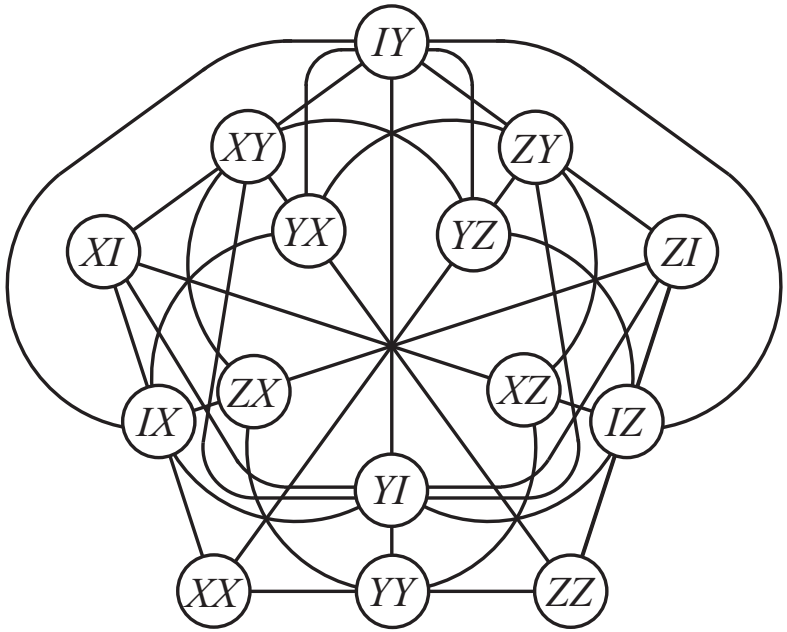

Case $n = 5$: geometric hyperplanes

$\mathcal{C}(\widetilde{D}_5)$ features 23 geometric hyperplanes:

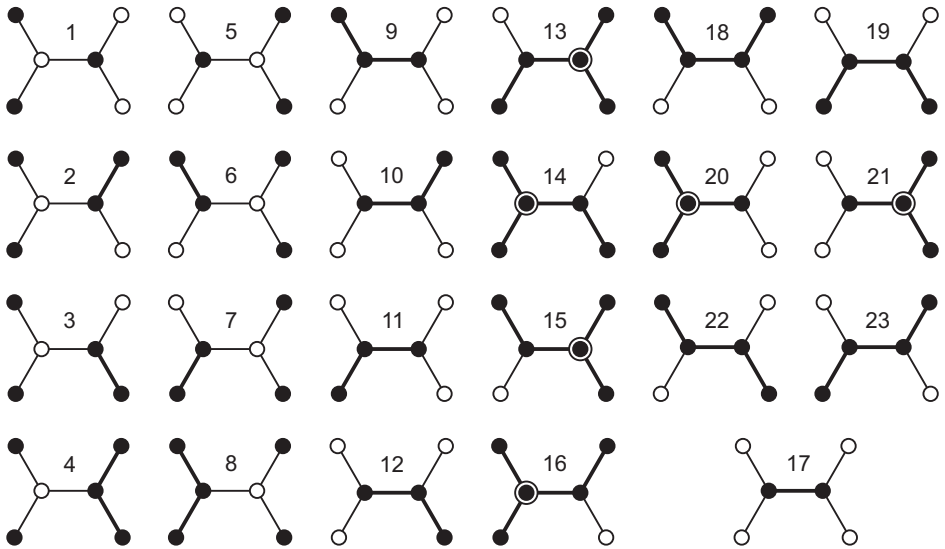

They can be split into two disjoint families, namely $\{H_1, H_2, \ldots, H_8\}$ and $\{H_9, H_{10}, \ldots, H_{23}\}$ according as they do not or do contain the line $\{2, 3\}$, respectively.

The former family can further be divided into two subfamilies, $\{H_1, H_2, H_3, H_4\}$ and $\{H_5, H_6, H_7, H_8\}$, depending on whether a hyperplane misses, respectively, point '2' or point '3'.

These splittings have a deep geometrical meaning once we see all 47 three-point Veldkamp lines $\mathcal{C}(\widetilde{D}_5)$ is found to possess.

Case $n = 5$: 12 Veldkamp lines

Twelve of them are generated by hyperplanes of the first family and they are given in the following table:

	H_1	H_2	H_3	H_4	H_5	H_6	H_7	H_8	H_{13}	H_{14}	H_{15}	H_{16}	H_{20}	H_{21}
1	+	+								+				
2	+		+									+		
3	+			+									+	
4		+	+										+	
5		+		+								+		
6			+	+						+				
7					+	+			+					
8					+		+				+			
9					+			+						+
10						+	+							+
11						+		+			+			
12							+	+	+					

As it is obvious from this table, the four hyperplanes of either subfamily define PG(2, 2), the Fano plane, with one line omitted; the latter being line $\{H_{14}, H_{16}, H_{20}\}$ for the first and $\{H_{13}, H_{15}, H_{21}\}$ for the second subfamily. We see that the Veldkamp points of the first/second Fano plane are those seven hyperplanes that contain H_1/H_5, and the two 'missing' lines consist of those three hyperplanes that contain H_{20}/H_{21}.

Case $n = 5$: 35 Veldkamp lines

The remaining 15 Veldkamp points (that are all geometric hyperplanes incorporating H_{17}, and 35 Veldkamp lines define a projective space isomorphic to PG$(3, 2)$; this space also contains two 'missing' lines (marked in italics in the next table) of the above-described Fano planes.

Case $n = 5$: 35 Veldkamp lines

	H_9	H_{10}	H_{11}	H_{12}	H_{13}	H_{14}	H_{15}	H_{16}	H_{17}	H_{18}	H_{19}	H_{20}	H_{21}	H_{22}	H_{23}
13	+	+									+				
14	+		+										+		
15	+			+											+
16	+				+				+						
17	+					+				+					
18	+						+					+			
19	+							+						+	
20		+	+											+	
21		+		+								+			
22		+			+					+					
23		+				+			+						
24		+					+								+
25		+						+					+		
26			+	+						+					
27			+		+							+			
28			+			+									+
29			+				+		+						
30			+					+			+				
31				+	+									+	
32				+		+							+		
33				+			+				+				
34				+				+	+						
35					+	+					+				
36					+		+						+		
37					+			+							+
38						+	+							+	
39						+		+				+			
40							+	+		+					
41									+	+	+				
42									+			+	+		
43									+					+	+
44										+		+		+	
45										+			+		+
46											+	+			+
47											+		+	+	

Case $n = 5$: full subgeometry

Summing up, the subgeometry of the Veldkamp space of $\mathcal{C}(\widetilde{D}_5)$ with lines of size three comprises the projective space PG(3, 2) and a couple of disjoint Fano planes, each sharing a line with this PG(3, 2). (It is also worth adding that in this case we have no exceptional Veldkamp point(s) since there is no geometric hyperplane lacking line $\{2, 3\}$.)

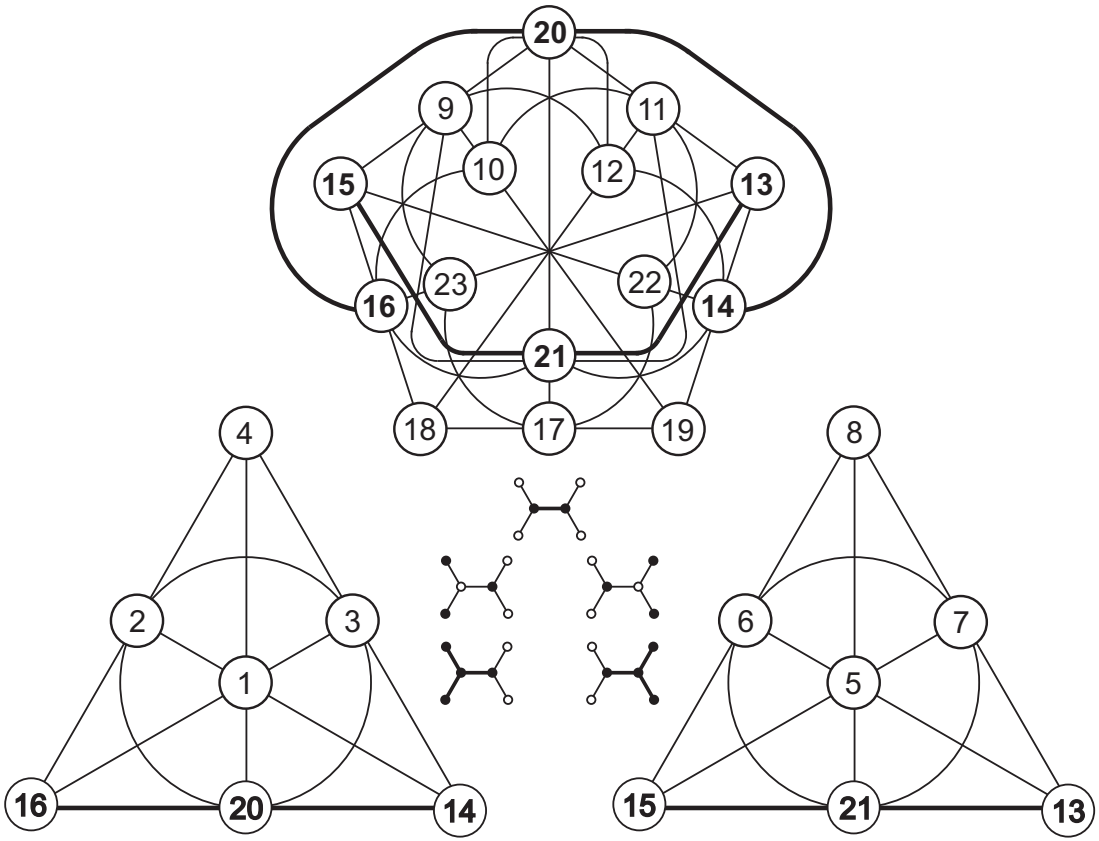

The central inset depicts those geometric hyperplanes each of which fully encodes all Veldkamp points of a particular subgeometry, namely of the PG(3, 2) (H_{17}, top), the two Fano planes (H_1 and H_5, middle) as well as of the two shared lines (H_{20} and H_{21}, bottom).

Case $n = 5$: two-qubit Pauli group

Next, pursuing the strategy of the preceding case, one labels six vertices of $\widetilde{D}_5$ by elements of the two-qubit Pauli group as

$$0 \to ZI,\ 1 \to XI,\ 2 \to YI,\ 3 \to IY,\ 4 \to IZ,\ 5 \to IX,$$

and gets the following bijection between the elements of the group and the points of the PG$(3, 2)$; this table also shows which elements of the two-qubit Pauli group are ascribed to the remaining eight points of the two Fano planes.

$\overline{\mathcal{P}}_2$	XY	YX	ZY	YZ	ZI	IZ	XI	IX	YY	XX	ZZ	IY	YI	XZ	ZX
PG$(3, 2)$	H_9	H_{10}	H_{11}	H_{12}	H_{13}	H_{14}	H_{15}	H_{16}	H_{17}	H_{18}	H_{19}	H_{20}	H_{21}	H_{22}	H_{23}
1st Fano		H_2		H_3					H_1				H_4		
2nd Fano	H_6		H_7						H_5			H_8			

Case $n = 5$: two-qubit Pauli group

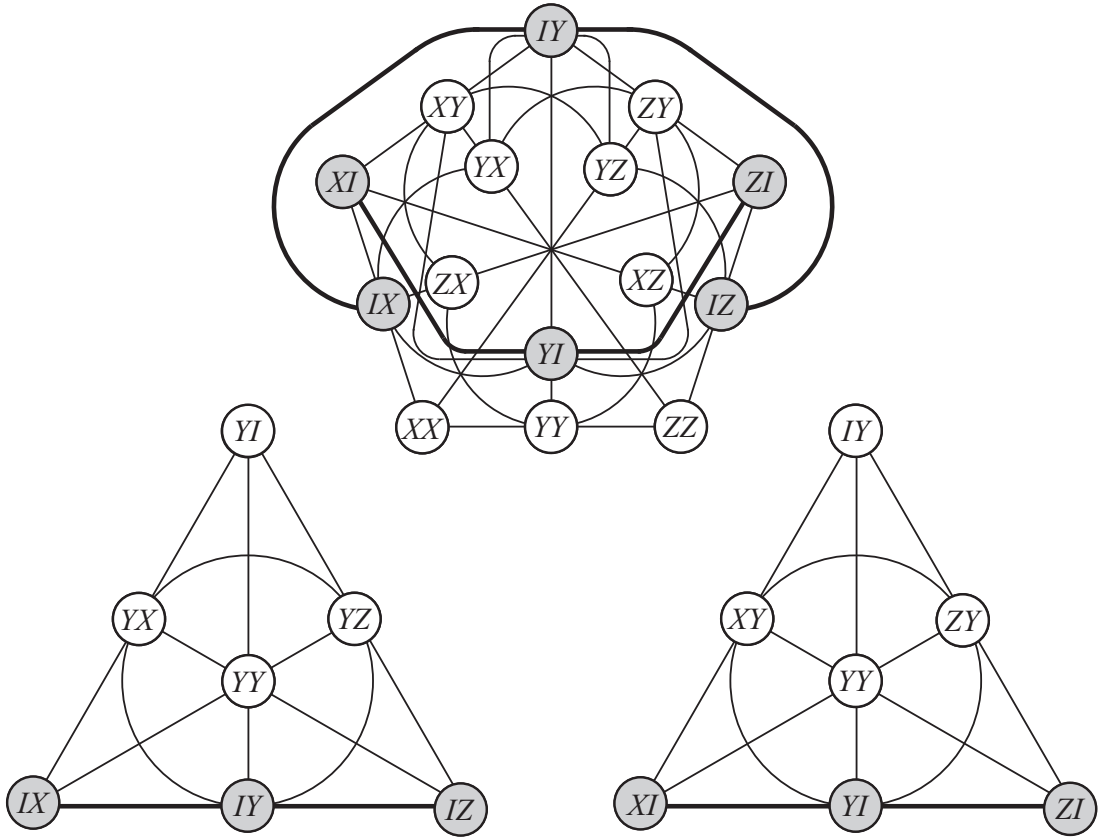

A general view of the projective subgeometries of the Veldkamp space of $\mathcal{C}(\widetilde{D}_5)$ in terms of the elements of the two-qubit Pauli group.

Case $n = 5$: two-qubit Pauli group

The bijection is of similar nature as the one of the $n = 4$ case: that is, a line of the PG$(3, 2)$ entails three group elements whose product is II, and a line of the distinguished copy of $W(3, 2)$ gathers a triple of mutually commuting elements.

Yet, it also features an interesting novelty due to the fact that our PG$(3, 2)$ has two distinguished lines that it shares with the two Fano planes. If we forget about the six group elements located on these two lines (highlighted by light shading in the previous figure) we shall find that the remaining nine elements form within the $W(3, 2)$ nothing but a 3×3 grid (or, what amounts to the same, a copy of the generalized quadrangle GQ$(2, 1)$).

Physical importance of this observation lies, as we saw before, with the fact that any such grid with the labeling inherited from that of its parent $W(3, 2)$ represents the so-called Mermin magic square.

Case $n = 6$: geometric hyperplanes

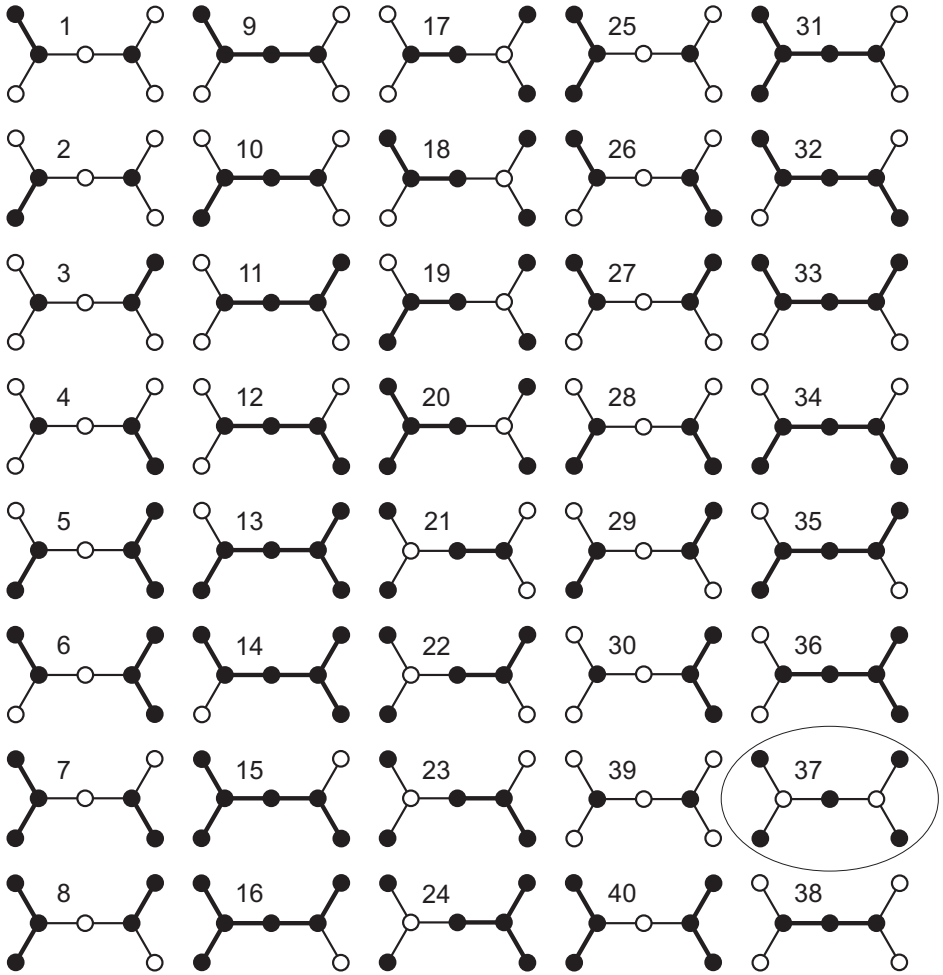

40 geometric hyperplanes of $\mathcal{C}(\widetilde{D}_6)$; an ellipse marks the (single) exceptional hyperplane.

Case $n = 6$: projective stratification of Veldkamp space

A detailed inspection of the previous figure leads to the following observations:

The smallest hyperplane, H_{39}, is contained in other 30 hyperplanes, which together yield 155 three-point Veldkamp lines and form the projective space isomorphic to PG$(4, 2)$.

This projective space also contains a distinguished copy of PG$(3, 2)$ that is defined by H_{38} and the other 14 hyperplanes containing it.

Then we have a pair of complementary Fano planes, one defined by seven hyperplanes containing H_{17}, the other by seven hyperplanes comprising H_{21}. Either of the two Fano planes shares a line with the distinguished copy of PG$(3, 2)$ (and, hence, also with the parent PG$(4, 2)$); it is the line defined by three hyperplanes containing H_{36} in the former and H_{31} in the latter case.

This already accounts for $155 + (2 \times 6) = 167$ Veldkamp lines. The remaining Veldkamp line is $\{H_{20}, H_{24}, H_{37}\}$, the joint of the two Fano planes, which is the *only* size-three Veldkamp line passing through the exceptional Veldkamp point H_{37}.

Case $n = 6$: projective stratification of Veldkamp space

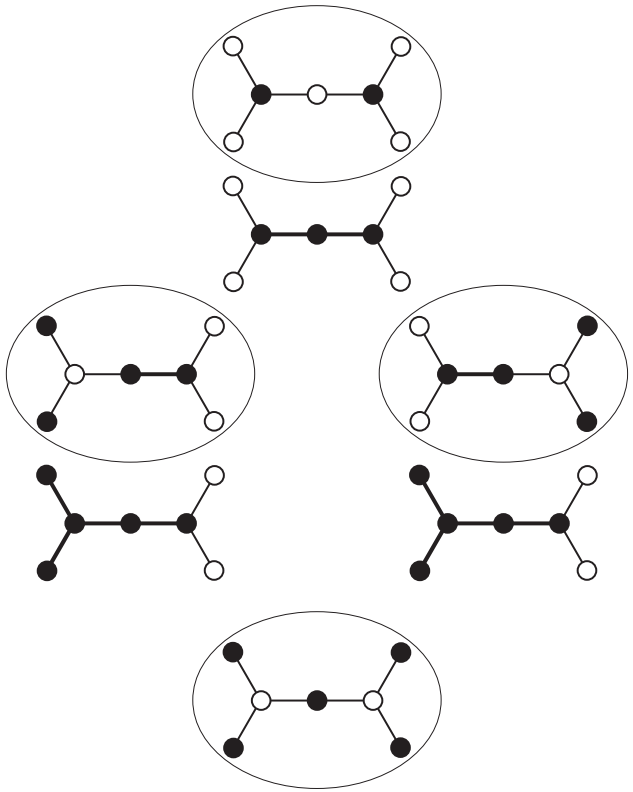

A symbolic structure of the Veldkamp space of $\mathcal{C}(\widetilde{D}_6)$. Each projective space (starting with the PG$(4, 2)$ at the top and ending with the 'exceptional' PG$(1, 2)$ at the bottom) is represented by a single hyperplane, viz. the one that fully determines the remaining hyperplanes defining the space in question. Marked by ellipses are those spaces that are not properly contained in any other space.

Case $n = 6$: projective stratification of Veldkamp space

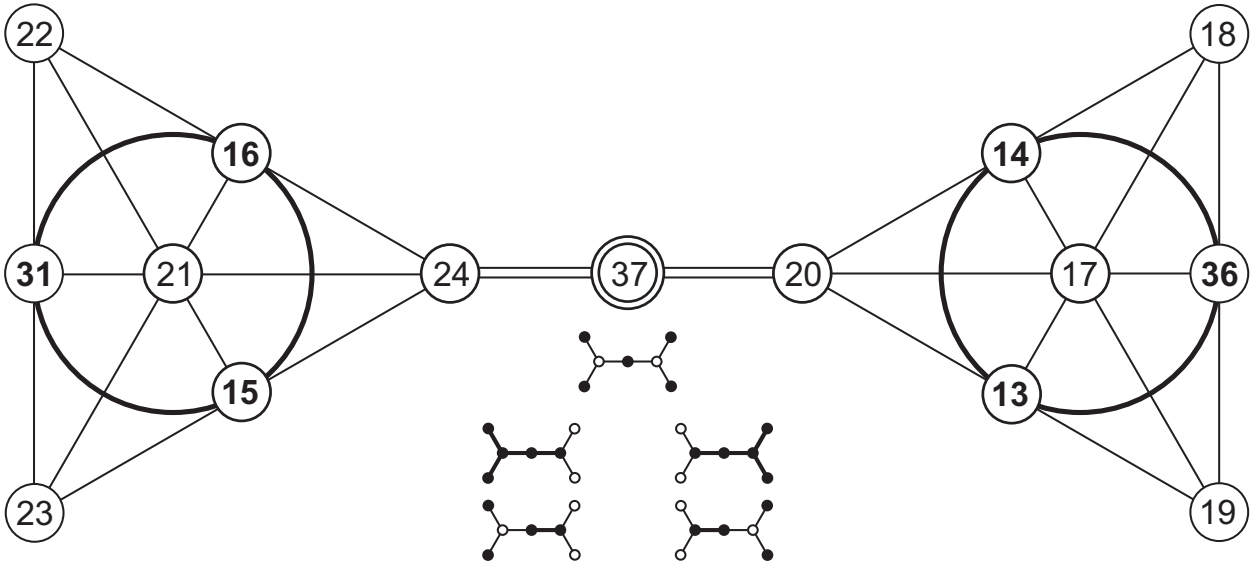

The two Fano planes and the exceptional Veldkamp line interconnecting them. The lines that also belong to the distinguished PG(3, 2) are drawn in boldface. (As before, the inset shows the representative hyperplanes for these projective geometries).

Case $n = 6$: two-qubit Pauli group

An interesting thing here happens when it comes to the relation with the two-qubit Pauli group, as we have now at our disposal two natural labelings of the vertices of $\widetilde{D}_6$, both featuring, unlike the previous two cases, also the identity element; in particular,

$$0 \to ZI,\ 1 \to XI,\ 2 \to YI,\ 3 \to II,\ 4 \to IY,\ 5 \to IZ,\ 6 \to IX,$$

and

$$0 \to ZI,\ 1 \to XI,\ 2 \to II,\ 3 \to YY,\ 4 \to II,\ 5 \to IZ,\ 6 \to IX.$$

These two labelings give

- *the same* labeling of the points of the distinguished PG$(3, 2)$, but
- *different* ones when the two interconnected Fano planes are concerned;

this difference is most pronounced for the exceptional Veldkamp line, as in the second case its three points acquire the same label, this being the identity element at that.

Case $n = 6$: two-qubit Pauli group

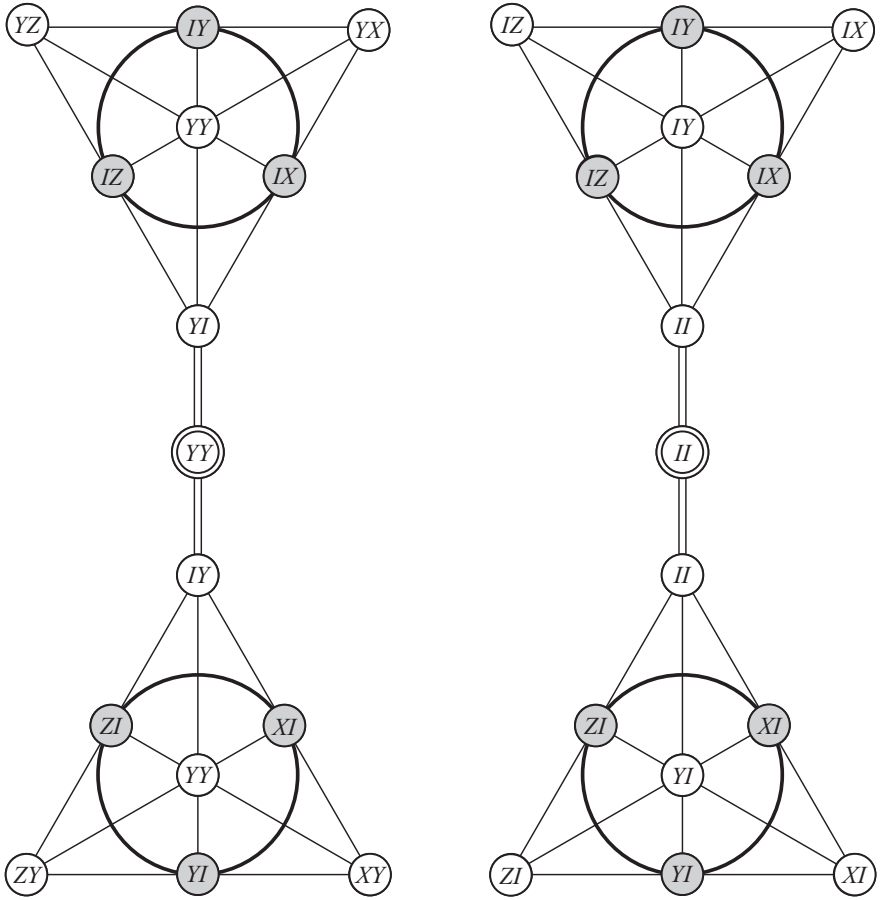

The pair of interconnected Fano planes in light of the two distinct two-qubit labelings.

Case $n = 7$: projective stratification of Veldkamp space

$\mathcal{C}(\widetilde{D}_7)$ is found to accommodate 64 geometric hyperplanes and 332 Veldkamp lines of size three, with the following hierarchical projective structure

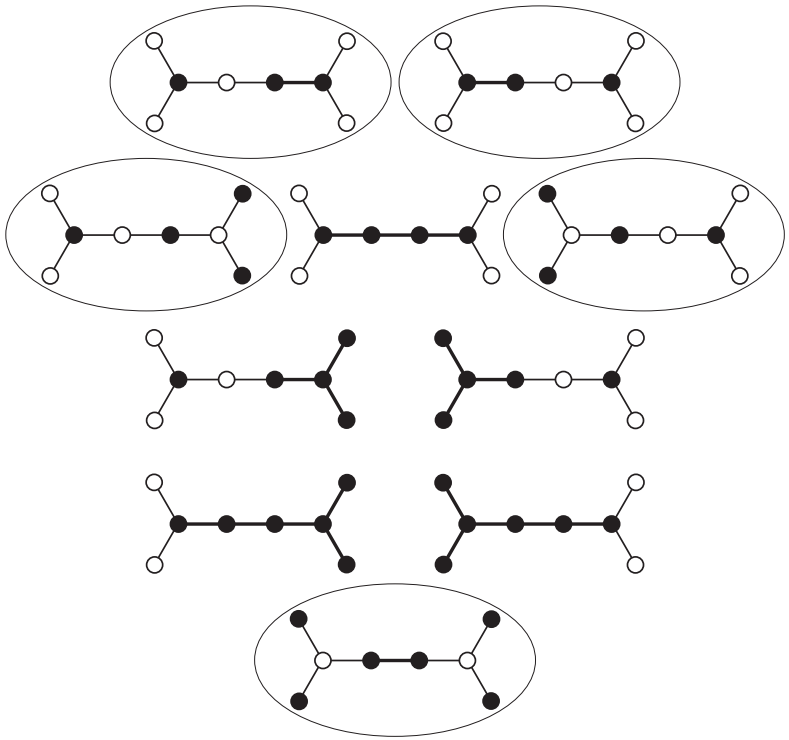

Figure: Stratification of the Veldkamp space of $\mathcal{C}(\widetilde{D}_7)$ in terms of projective spaces it contains.

Case $n = 7$: projective stratification of Veldkamp space

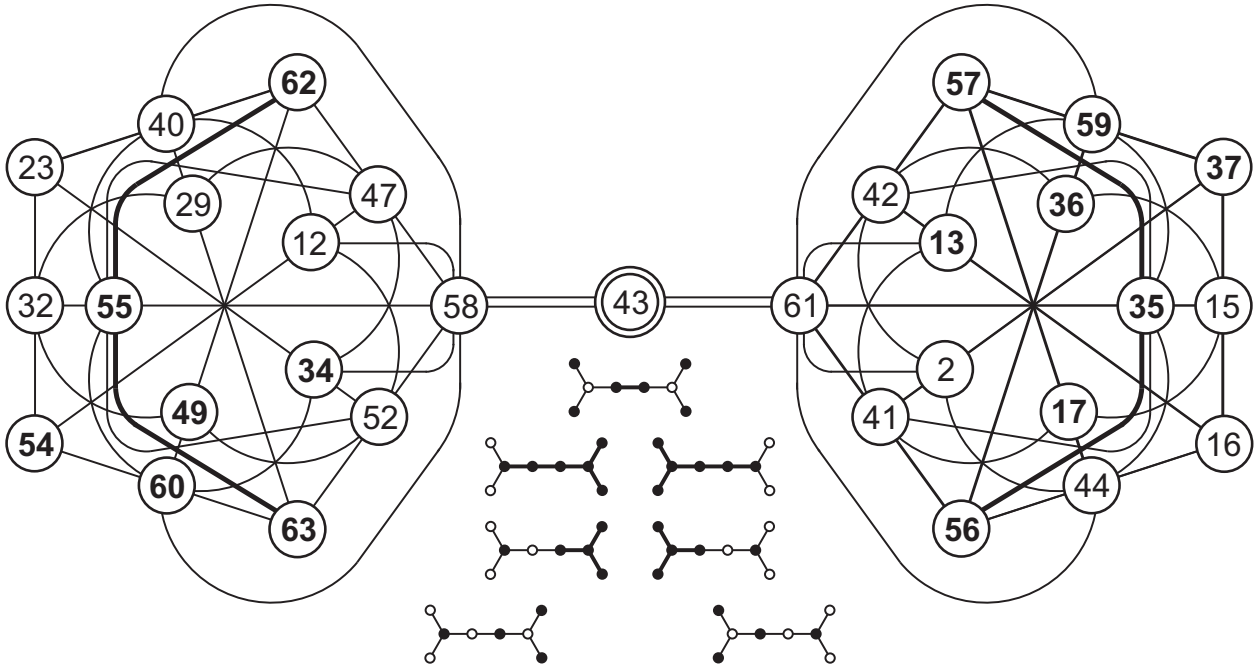

The left and right PG(3, 2)s connected by the exceptional Veldkamp line. The seven points in either of these spaces that are numbered in boldface represent the Fano plane lying also in the corresponding PG(4, 2); the line of this Fano plane that also belongs to the distinguished PG(3,2) is drawn thick. (As before, the inset depicts the representative hyperplane for each of the projective spaces mentioned.)

Case $n = 7$: two-qubit Pauli group

Regarding a relation with the two-qubit Pauli group, we again see close parallels with the $n = 6$ case. For not only do we have again two natural labellings of the vertices of $\widetilde{D}_7$,

$$0 \to ZI,\ 1 \to XI,\ 2 \to YI,\ 3 \to II,\ 4 \to II,\ 5 \to IY,\ 6 \to IZ,\ 7 \to IX,$$

and

$$0 \to ZI,\ 1 \to XI,\ 2 \to II,\ 3 \to YI,\ 4 \to IY,\ 5 \to II,\ 6 \to IZ,\ 7 \to IX,$$

but these also give identical labellings of the distinguished PG$(3, 2)$, furnishing the same prominent copy of the Mermin magic square; in addition, as illustrated in the next figure, the two labelings of the exceptional Veldkamp line are the same as those of its $n = 6$ counterpart.

Case $n = 7$: two-qubit Pauli group

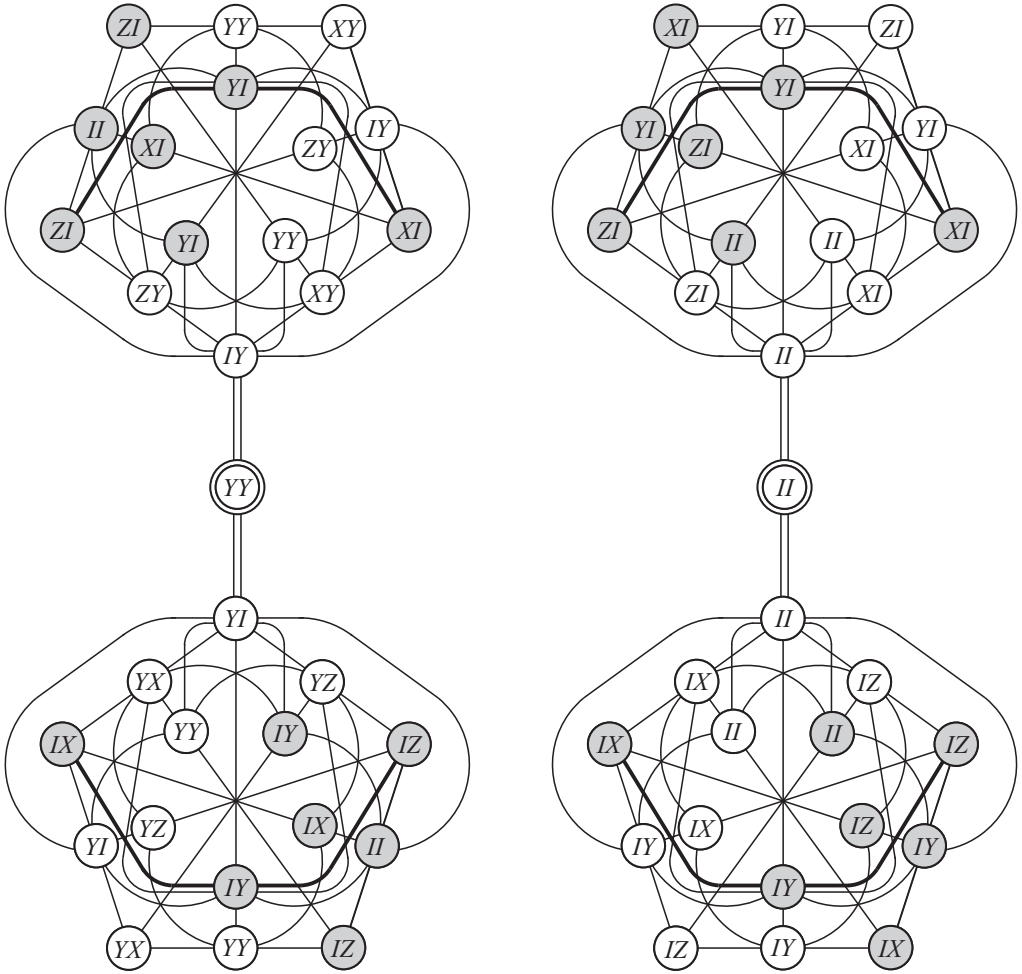

The interconnected left and right PG(3, 2)s in terms of the two two-qubit labelings.

Case $n = 8$: projective layering

The Veldkamp space of $\mathcal{C}(\widetilde{D}_8)$ has 105 points and 876 size-three lines, exhibiting the following projective layering:

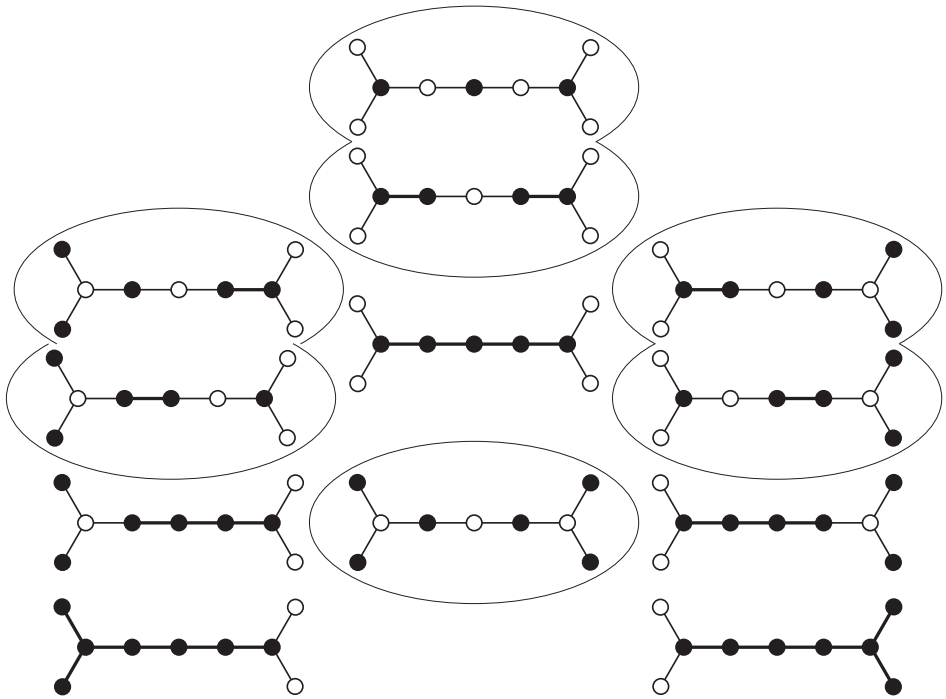

From the figure we find out that this Veldkamp space includes one PG(5, 2) (1st row) and one PG(4, 2) (2nd row), the two having the distinguished PG(3, 2) in common (3rd row, middle). Next, we have here other four PG(3, 2)s (3rd row, left- and right-hand side), forming two complementary pairs. As before, there are two special, disjoint lines in the distinguished PG(3, 2), which the latter shares with either of PG(3, 2)s in both complementary pairs.

Case $n = 8$: exceptional Fano plane

However, the most interesting object for us is here the Fano plane represented by the hyperplane depicted in the middle of the 4th row of the figure.

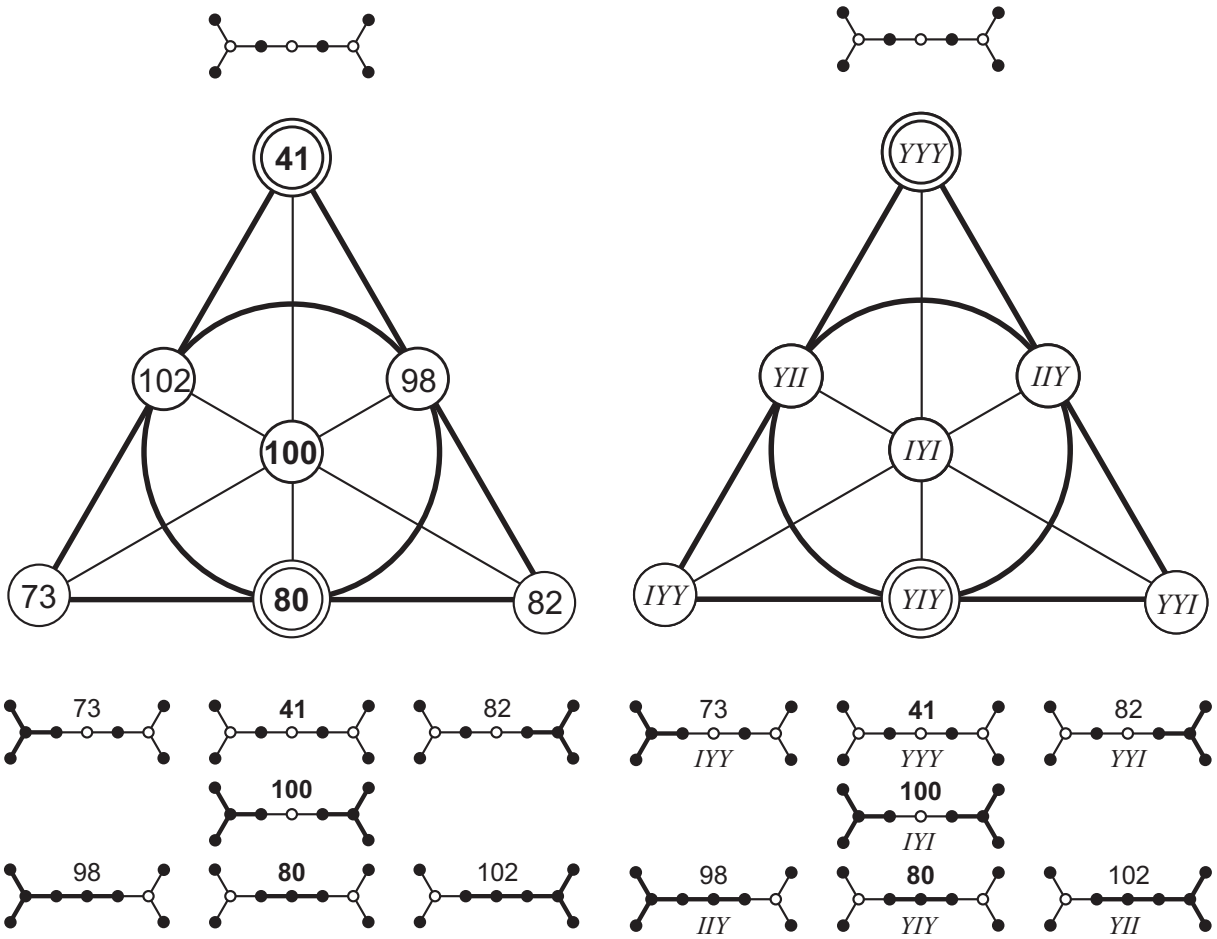

The explicit structure of the unique Fano plane whose two points are represented by the two exceptional hyperplanes of $\mathcal{C}(\widetilde{D}_8)$ and the associated three-qubit labeling of its points. The four heavy lines and the six points on them form a Pasch configuration.

Case $n = 8$: three qubit-labeling

This case is remarkable in that the most natural labeling of the (nine) vertices of $\widetilde{D}_8$ employs elements of the *three*-qubit Pauli group, in particular

$$0 \to XII,\ 1 \to ZII,\ 2 \to YII,\ 3 \to IXI,\ 4 \to IYI,\ 5 \to IZI,\ 6 \to IIY,\ 7 \to IIX,\ 8 \to IIZ.$$

It represents no difficulty to verify that this labeling yields a one-to-one correspondence between 63 elements of the three-qubit Pauli group and 63 points of the PG$(5, 2)$. Under this correspondence, our distinguished PG$(3, 2)$ acquires the three-qubit lettering as follows:

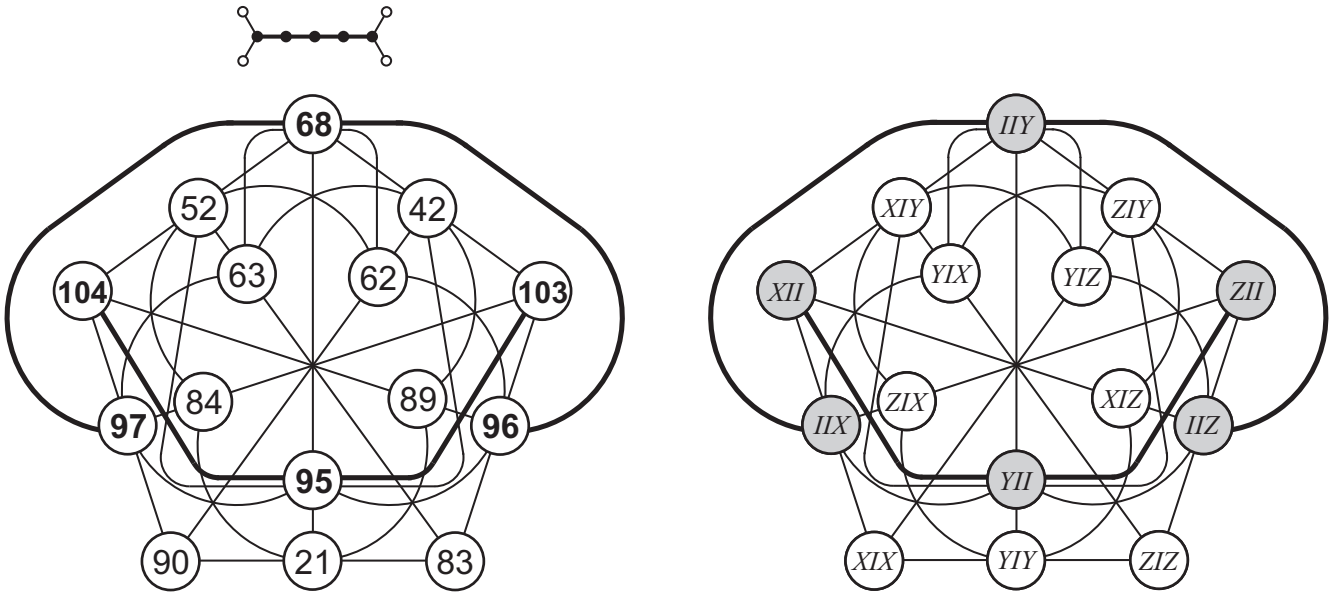

One explicitly sees a bijection between 15 points of this PG$(3, 2)$ and 15 elements of a two-qubit subgroup of the three-qubit Pauli group, the geometry of the subgroup encoded in the selected copy of $W(3, 2)$ and a three-qubit version of the Mermin magic square.

Pseudo-Veldkamp spaces

GQ(2,2): tricentric triads (form complementary pairs)

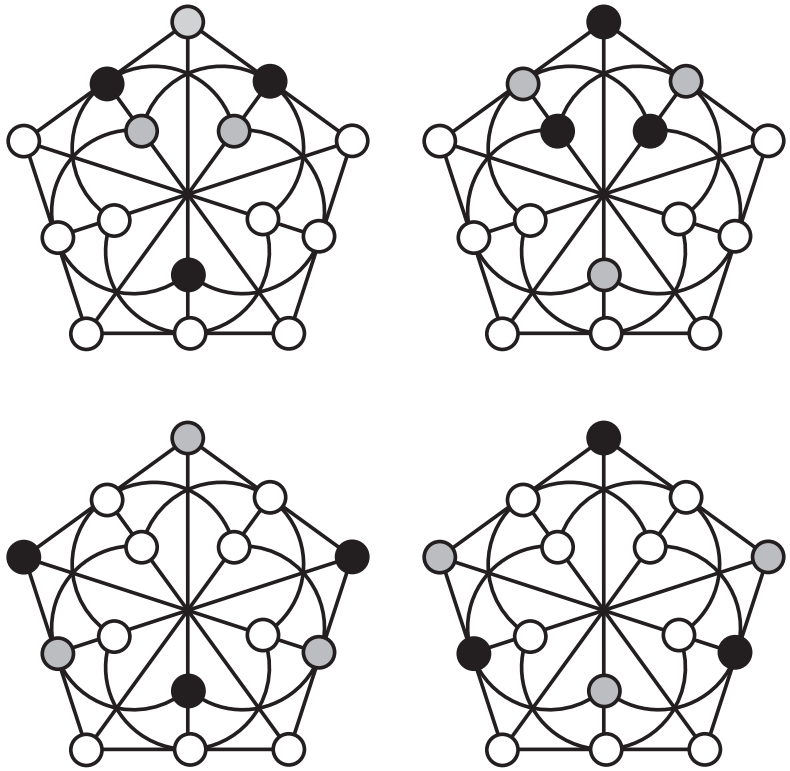

On pseudo-Veldkamp spaces: Pasch configuration

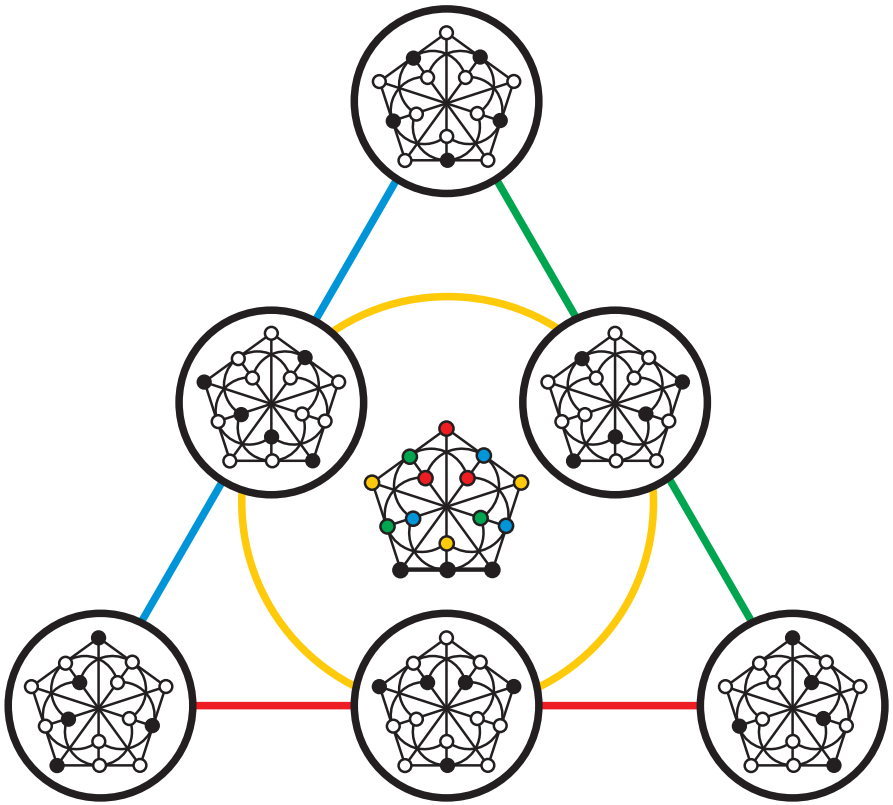

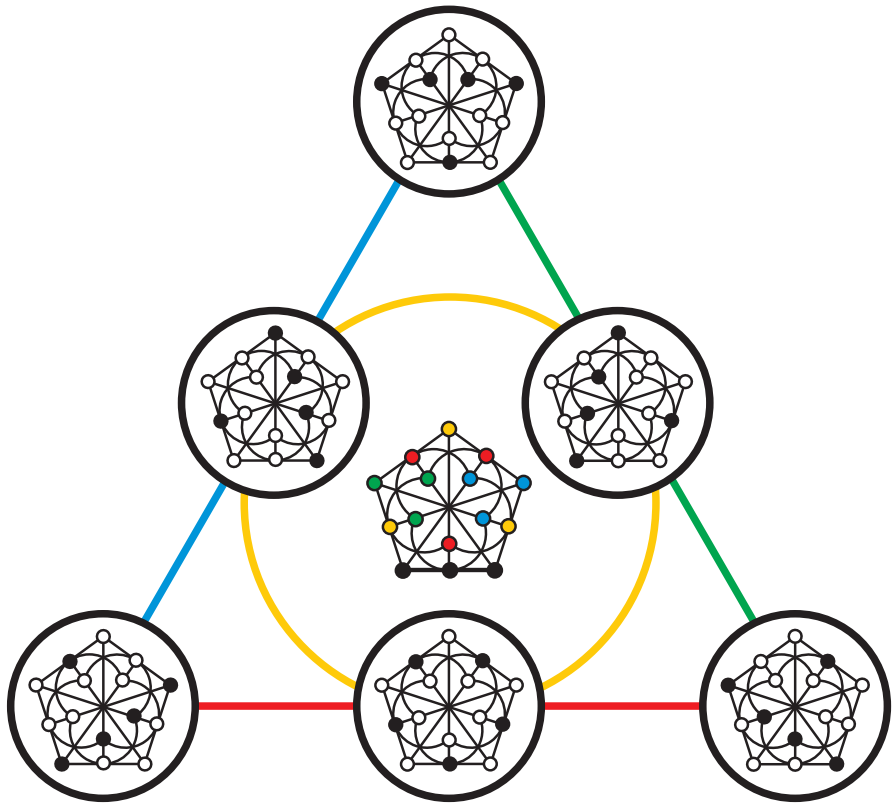

Points of the Pasch configuration are the 6 *ovoids* of GQ(2,2). Three ovoids forming a line are such that they have the same tricentric triad of GQ(2,2) in their complements. As tricentric triads come in complementary pairs, we get this way two twin Pasch configurations that originate from each other by a Pasch switch/trade.

On pseudo-Veldkamp spaces: complete five-lateral

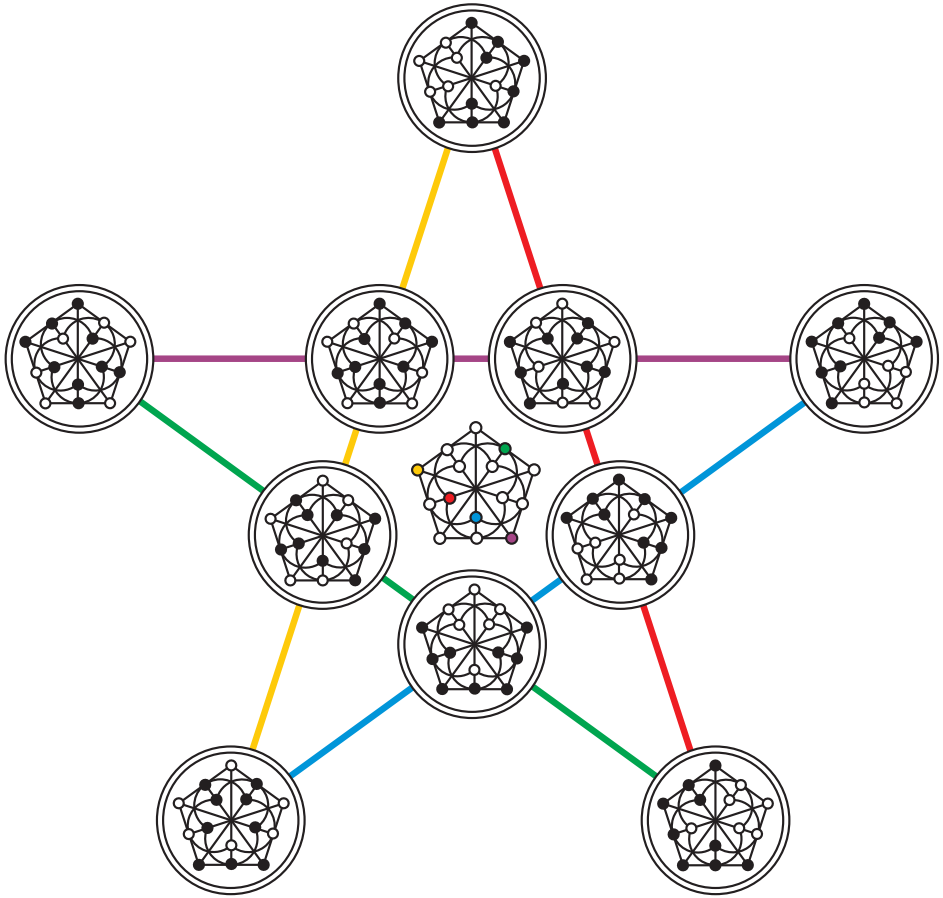

Points of the five-lateral are the 10 *grids* of GQ(2,2). Four grids forming a line are such that there is only one point of GQ(2,2) that does not belong to any of them, the five single points forming an ovoid of GQ(2,2).

On pseudo-Veldkamp spaces: complete six-lateral

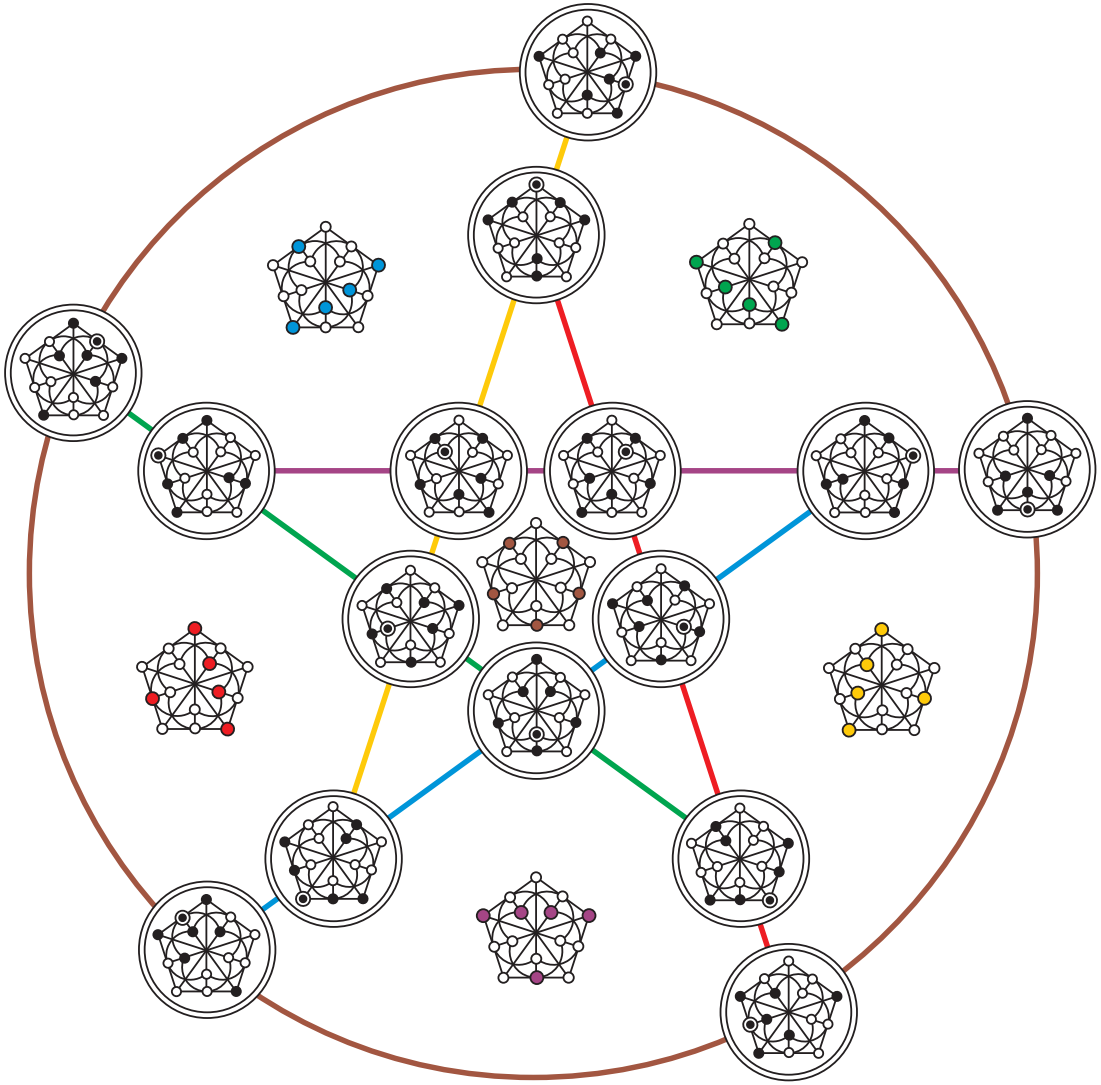

Points of the six-lateral are the 15 *perps* of GQ(2,2). Five perps forming a line are such that their deep points form an ovoid of GQ(2,2).

On pseudo-Veldkamp spaces: Steiner-Plücker twins

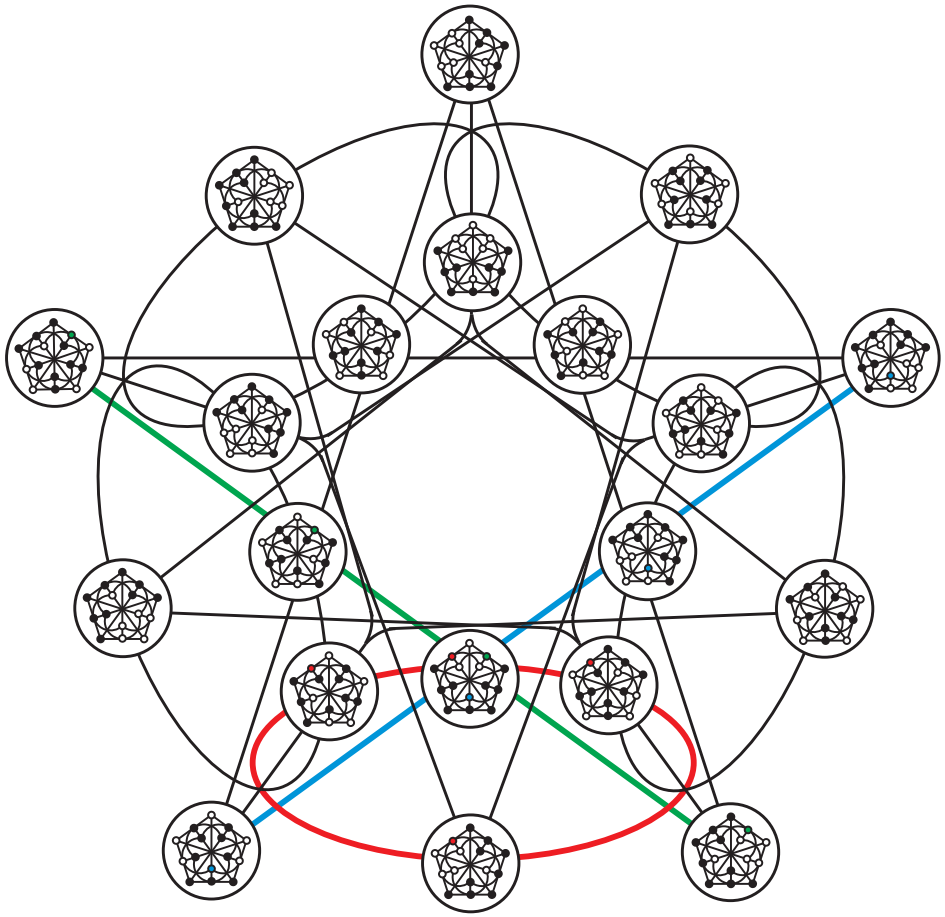

Points of the SP configuration are the 10 *grids* of GQ(2,2), two antipodal points being represented by the same grid. Four grids forming a line are such that there is only one point of GQ(2,2) that does not belong to any of them; the three single points that correspond to three concurrent lines of the SP configuration form a tricentric triad of GQ(2,2).

On pseudo-Veldkamp spaces: Steiner-Plücker twins

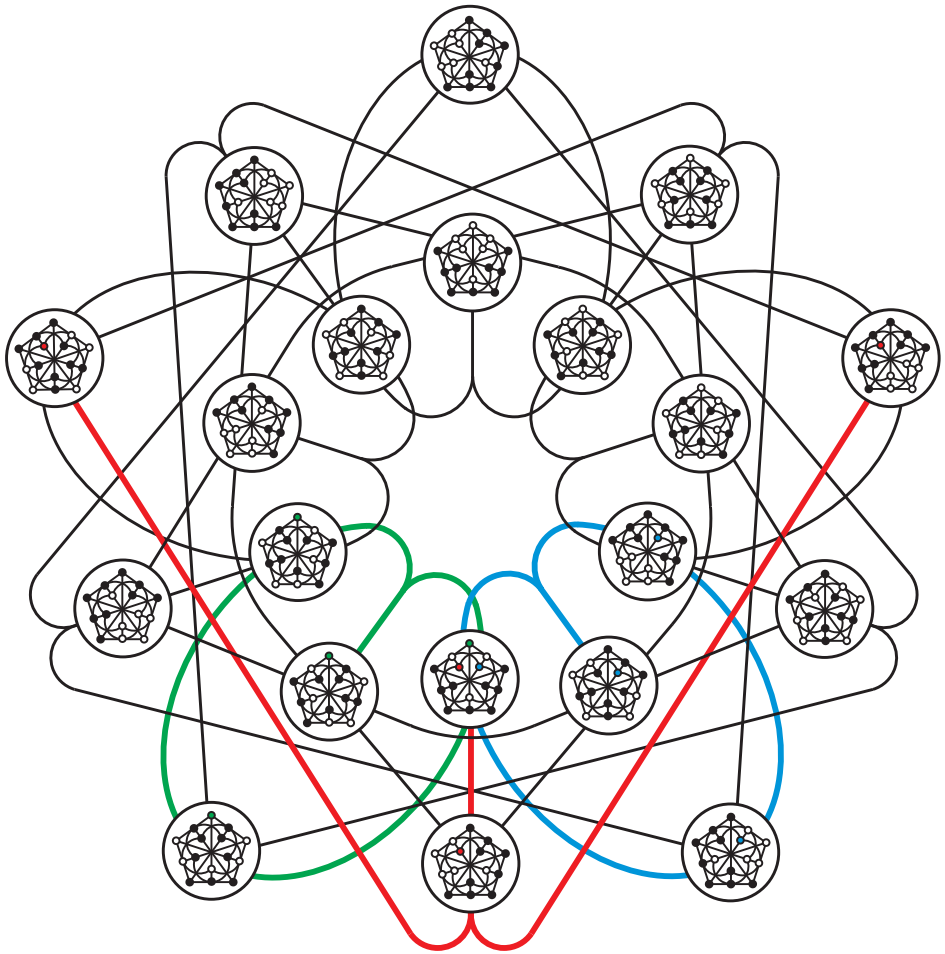

Points of the SP configuration are the 10 *grids* of GQ(2,2), two antipodal points being represented by the same grid. Four grids forming a line are such that there is only one point of GQ(2,2) that does not belong to any of them; the three single points that correspond to three concurrent lines of the SP configuration form a tricentric triad of GQ(2,2).

Relevant references

Saniga, M., Havlicek, H., Planat, M., and Pracna, P.: 2008, Twin "Fano-Snowflakes" over the Smallest Ring of Ternions, *Symmetry, Integrability and Geometry: Methods and Applications* **4**, Paper 050, 7 pages; (arXiv:0803.4436).

Havlicek, H., and Saniga, M.: 2009, Vectors, Cyclic Submodules and Projective Spaces Linked with Ternions, *Journal of Geometry* **92**, 79–90; (arXiv:0806.3153).

Saniga, M., and Pracna, P.: 2010, Space versus Time: Unimodular versus Non-Unimodular Projective Ring Geometries?, *Journal of Cosmology* **4**, 719–735; (arXiv:0808.0402).

Saniga, M., Lévay, P., Planat, M., and Pracna, P.: 2010, Geometric Hyperplanes of the Near Hexagon $\mathsf{L}_3 \times$ GQ(2, 2), *Letters in Mathematical Physics* **91**, 93–104; (arXiv:0908.3363).

Saniga, M., Green, R. M., Lévay, P., Pracna, P., and Vrana, P.: 2010, The Veldkamp Space of GQ(2, 4), *International Journal of Geometric Methods in Modern Physics* **7**(7), 1133–1145; (arXiv:0903.0715).

Saniga, M.: 2011, On the Veldkamp Space of GQ(4, 2), *International Journal of Geometric Methods in Modern Physics* **8**(1), 39–47; (arXiv:1001.0659).

Saniga, M., Havlicek, H., Holweck, F., Planat, M., and Pracna, P.: 2015, Veldkamp-Space Aspects of a Sequence of Nested Binary Segre Varieties, *Annales de l'Institut Henri Poincaré D: Combinatorics, Physics and their Interactions* **2**(3), 309–333; (arXiv:1403.6714).

Saniga, M., Holweck, F., and Pracna, P.: 2015, From Cayley-Dickson Algebras to Combinatorial Grassmannians, *MDPI: Mathematics* **3**(4), 1192–1221; (arXiv:1405.6888).

Saniga, M., Holweck, F., and Pracna, P.: 2017, Veldkamp Spaces: From (Dynkin) Diagrams to (Pauli) Groups, *International Journal of Geometric Methods in Modern Physics* **14**(5), 1750080, 23 pages; (arXiv:1605. 02001).

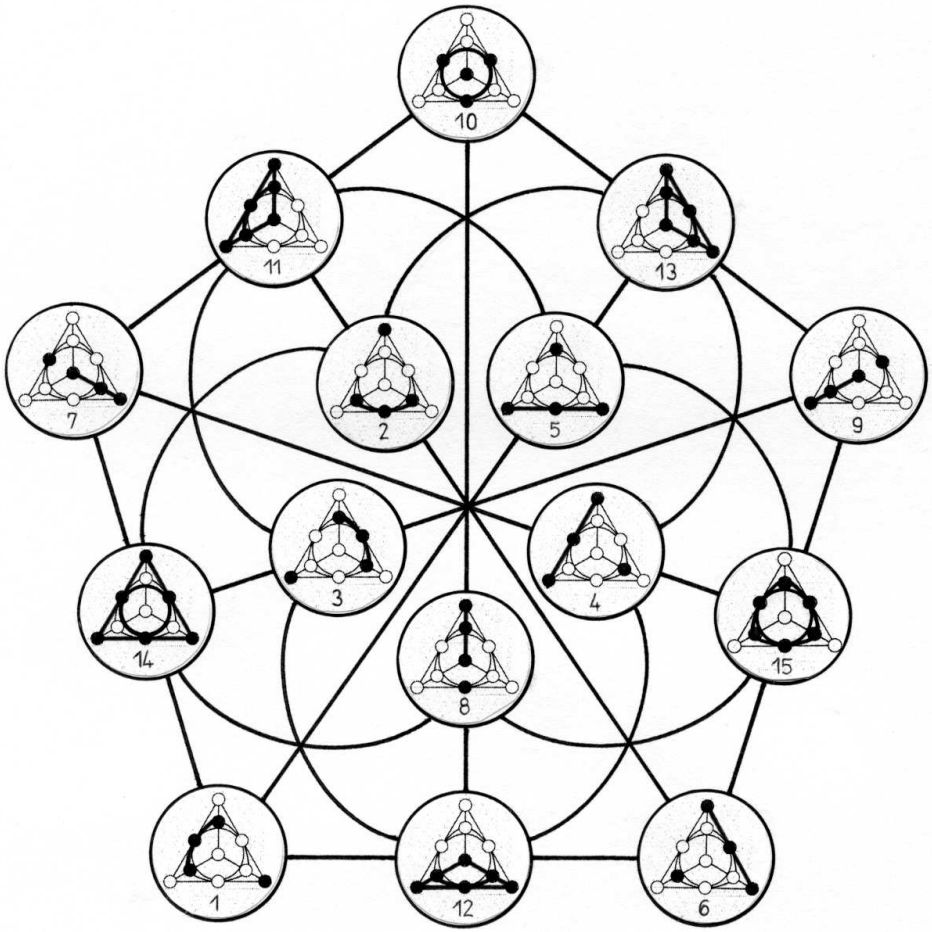

Thank you for your attention!